

Bayesian Mosaic: Parallelizable Composite Posterior

Ye Wang and David B. Dunson
Department of Statistical Science
Duke University

Abstract

This paper proposes *Bayesian mosaic*, a parallelizable composite posterior, for scalable Bayesian inference on a broad class of multivariate discrete data models. Sampling is embarrassingly parallel since *Bayesian mosaic* is a multiplication of component posteriors that can be independently sampled from. Analogous to composite likelihood methods, these component posteriors are based on univariate or bivariate marginal densities. Utilizing the fact that the score functions of these densities are unbiased, we show that *Bayesian mosaic* is consistent and asymptotically normal under mild conditions. Since the evaluation of univariate or bivariate marginal densities can rely on numerical integration, sampling from *Bayesian mosaic* bypasses the traditional data augmented Markov chain Monte Carlo (DA-MCMC) method, which has a provably slow mixing rate when data are imbalanced. Moreover, we show that sampling from *Bayesian mosaic* has better scalability to large sample size than DA-MCMC. The method is evaluated via simulation studies and an application on a citation count dataset.

Key Words: Big data; Composite likelihood; Discrete data; Embarrassingly parallel; Hierarchical model; High-dimensional; Latent Gaussian

1 INTRODUCTION

There is great interest in designing flexible models for multivariate discrete data. A common strategy is to define a generalized linear model (GLM) for each variable, with dependence in the different variables induced through including multivariate latent variables in the GLMs. Alternatively, discrete data can be directly linked to the latent variables via some link functions. A popular choice for the latent variable distribution is the multivariate Gaussian due to simplicity in modeling the dependence structure. For instance, multivariate Poisson regression with the underlying intercepts modeled jointly as a Gaussian has been widely used in accident analysis [Ma et al., 2008, El-Basyouny et al., 2014]. Canale and Dunson [2011] proposed a multivariate count model that handles both over-dispersion and under-dispersion. This model uses a rounding function to directly link the multivariate count data to a latent Gaussian. We term these models as multivariate latent Gaussian models. Unfortunately, despite their great flexibility, the usage of this class of models is limited by the computationally challenging model fitting.

The challenge is due partially to the fact that likelihood functions marginalizing out the latent variables lack analytic forms. Hence, Bayesian inference is usually done via data augmented Markov chain Monte Carlo (DA-MCMC) algorithms that sample both the latent variables and the model parameters from their joint posterior. However, it is well known that posterior dependence between the latent variables and the model parameters can substantially slow down the mixing rate of the Markov chain. In fact, Johndrow et al. [2016] has shown that the mixing rate can be so slow that the DA-MCMC sampler cannot generate any reliable posterior samples when the data are severely imbalanced (e.g., excessive zeros in count data).

One possible solution is to bypass sampling entirely using one of the following two strategies. The first is the integrated nested Laplace approximation (INLA), which is designed for latent Gaussian models that have a small number of parameters remaining after marginalizing out the latent variables [Rue et al., 2009]. Although INLA has had excellent performance in specialized settings, in many applications, there are moderate to large numbers of population parameters, ruling out such approaches. Another strategy is the so-called variational approximations [Attias, 2000, Jaakkola and Jordan, 2000], which introduce an approximate posterior with a factorized form. One then optimizes the parameters of this approximate posterior to minimize its Kullback-Leibler divergence from the exact posterior. However, in gen-

eral one has no idea how accurate this approximation is and additionally it is well known that it often substantially underestimates the true posterior covariance.

We propose *Bayesian mosaic*, which is a surrogate posterior derived by multiplying a collection of component posteriors. Unlike variational approximations, where one has to choose the variational class and optimize its parameters, the construction of *Bayesian mosaic* is automatically determined by the data distribution. It is related to the composite likelihood approach [Cox and Reid, 2004] with its component posteriors being based on univariate and bivariate marginal distributions. However, *Bayesian mosaic* is different from Bayesian composite likelihood methods [Pauli et al., 2011] in that it has an easy-to-sample multiplicative form while a posterior density induced by a composite likelihood does not. Utilizing that these marginal densities have unbiased score functions, we have shown that *Bayesian mosaic* is consistent and asymptotically normal under mild conditions. It is applicable to a class of *mosaic-type* data distributions that covers and is much broader than the class of multivariate latent Gaussian models mentioned earlier.

We also propose an efficient parallel sampling strategy utilizing the posterior dependence structure induced by the multiplicative form. This parallelization is substantially different from standard parallel MCMC algorithms which are based on partitions of the dataset [Wang and Dunson, 2013, Scott et al., 2016]. The sparse dependence structure of *Bayesian mosaic* allows us to directly sample from each component posterior independently. Moreover, we have shown that the asymptotic per-iteration computational complexity of sampling from *Bayesian mosaic* is linear in the cardinality of the observed data, which is in general much smaller than the sample size. On the other hand, the per-iteration computational complexity of DA-MCMC is linear in the sample size.

The remainder of the paper is organized as follows. §2 provides definitions and the sampling strategy. §3 provides theories on the richness of the *mosaic-type* class and asymptotic properties of *Bayesian mosaic*. The performance is demonstrated via both simulation studies and an application on a citation network dataset in §4.

2 Bayesian Mosaic

We start by introducing notation that will be used throughout the paper. Before presenting the formal definition, we will first motivate the proposed method by introducing a class of multivariate latent Gaussian models and describing computational issues DA-MCMC algorithms encounter in fitting these models. After defining *Bayesian mosaic*, we present a sampling algorithm and a post-processing method to handle parameter constraints. We end the section by generalizing *Bayesian mosaic* to dependent data.

2.1 Notations

We represent vectors by lower case letters and matrices by capital letters, both in a boldface font. Unless otherwise stated, all vectors will be column vectors. We use \mathbb{R} to denote the set of all real numbers, \mathbb{N}_0 the nonnegative integers, \mathbb{N}_1 the positive integers and $\|\cdot\|$ the Euclidean norm. For $d \in \mathbb{N}_1$, $\boldsymbol{\theta} \in \mathbb{R}^d$ and $\delta > 0$, we define a radius- δ ball of $\boldsymbol{\theta}$ at $\boldsymbol{\theta}_0$ as $\mathcal{B}_{\boldsymbol{\theta}}(\boldsymbol{\theta}_0, \delta) = \{\boldsymbol{\theta} : \|\boldsymbol{\theta} - \boldsymbol{\theta}_0\| < \delta\}$. For succinctness, we denote the multiple integral of a multivariate function $g(\mathbf{y})$ as

$$\int g(\mathbf{y})d\mathbf{y} = \int \cdots \int g(y_1, \dots, y_p)dy_1 \cdots dy_p.$$

We will always use f to denote a density function and ℓ to denote a log-density function. The density function will be presented in a conditional style, e.g., $f(\mathbf{y}|\boldsymbol{\theta})$, where $\boldsymbol{\theta}$ are the model parameters. Given that \mathbf{y} follows some distribution $P_{\boldsymbol{\theta}}$ with a density function $f(\mathbf{y}|\boldsymbol{\theta})$, we use $\mathbb{E}_{\boldsymbol{\theta}}g(\mathbf{y})$ to denote the expectation of $g(\mathbf{y})$. More specifically,

$$\mathbb{E}_{\boldsymbol{\theta}}g(\mathbf{y}) = \int g(\mathbf{y})f(\mathbf{y}|\boldsymbol{\theta})d\mathbf{y}.$$

We use $\phi(\mathbf{x}|\boldsymbol{\mu}, \boldsymbol{\Sigma})$ to denote the density function of a Gaussian distribution with mean $\boldsymbol{\mu}$ and covariance $\boldsymbol{\Sigma}$, and use $\Phi(U|\boldsymbol{\mu}, \boldsymbol{\Sigma})$ to denote its cdf function:

$$\begin{aligned} \phi(\mathbf{x}|\boldsymbol{\mu}, \boldsymbol{\Sigma}) &= |2\pi\boldsymbol{\Sigma}|^{-1/2} \exp\left\{-\frac{(\mathbf{x} - \boldsymbol{\mu})^\top \boldsymbol{\Sigma}^{-1}(\mathbf{x} - \boldsymbol{\mu})}{2}\right\}, \\ \Phi(U|\boldsymbol{\mu}, \boldsymbol{\Sigma}) &= \int_U \phi(\mathbf{x}|\boldsymbol{\mu}, \boldsymbol{\Sigma})d\mathbf{x}. \end{aligned}$$

For better representation of the higher-order remainder of the Taylor expansion for multivariate functions, we adopt the notations of Folland [2005].

For any $d \in \mathbb{N}_1$, a d -dimensional *multi-index* $\boldsymbol{\alpha}$ for $\mathbf{x} = (x_1, \dots, x_d)^\top \in \mathbb{R}^d$ is defined as a d -tuple of nonnegative integers, i.e., $\boldsymbol{\alpha} = (\alpha_1, \dots, \alpha_d)$, where $\alpha_j \in \mathbb{N}_0$ for $j = 1, \dots, d$. We further define

$$|\boldsymbol{\alpha}| = \sum_{j=1}^d \alpha_j, \quad \boldsymbol{\alpha}! = \prod_{j=1}^d \alpha_j!, \quad \mathbf{x}^\boldsymbol{\alpha} = \prod_{j=1}^d x_j^{\alpha_j}, \quad \partial^\boldsymbol{\alpha} g(\mathbf{x}) = \frac{\partial^{|\boldsymbol{\alpha}|} g(\mathbf{x})}{\partial x_1^{\alpha_1} \dots \partial x_d^{\alpha_d}}.$$

We will also use the following vector calculus notation to ease our representation of the gradient vector and the Hessian matrix. Considering two vectors $\boldsymbol{\eta} = (\eta_1, \dots, \eta_{d_\eta})^\top$, $\boldsymbol{\zeta} = (\zeta_1, \dots, \zeta_{d_\zeta})^\top$ and some function $g(\boldsymbol{\eta}, \boldsymbol{\zeta})$, we denote the gradient of $f(\boldsymbol{\eta}, \boldsymbol{\zeta})$ w.r.t. $\boldsymbol{\eta}$ as

$$\nabla_{\boldsymbol{\eta}} g(\boldsymbol{\eta}, \boldsymbol{\zeta}) = \left[\frac{\partial g(\boldsymbol{\eta}, \boldsymbol{\zeta})}{\partial \eta_1}, \dots, \frac{\partial g(\boldsymbol{\eta}, \boldsymbol{\zeta})}{\partial \eta_{d_\eta}} \right]^\top,$$

and the gradient of $g(\boldsymbol{\eta}, \boldsymbol{\zeta})$ w.r.t. $\boldsymbol{\eta}$ and $\boldsymbol{\zeta}$ as

$$\nabla_{\boldsymbol{\eta}, \boldsymbol{\zeta}} g(\boldsymbol{\eta}, \boldsymbol{\zeta}) = \left[\frac{\partial g(\boldsymbol{\eta}, \boldsymbol{\zeta})}{\partial \eta_1}, \dots, \frac{\partial g(\boldsymbol{\eta}, \boldsymbol{\zeta})}{\partial \eta_{d_\eta}}, \frac{\partial g(\boldsymbol{\eta}, \boldsymbol{\zeta})}{\partial \zeta_1}, \dots, \frac{\partial g(\boldsymbol{\eta}, \boldsymbol{\zeta})}{\partial \zeta_{d_\zeta}} \right]^\top.$$

We further define

$$\nabla_{\boldsymbol{\zeta}} \nabla_{\boldsymbol{\eta}} g(\boldsymbol{\eta}, \boldsymbol{\zeta}) = \begin{bmatrix} \frac{\partial^2 g(\boldsymbol{\eta}, \boldsymbol{\zeta})}{\partial \eta_1 \partial \zeta_1} & \dots & \frac{\partial^2 g(\boldsymbol{\eta}, \boldsymbol{\zeta})}{\partial \eta_1 \partial \zeta_{d_\zeta}} \\ \vdots & & \vdots \\ \frac{\partial^2 g(\boldsymbol{\eta}, \boldsymbol{\zeta})}{\partial \eta_{d_\eta} \partial \zeta_1} & \dots & \frac{\partial^2 g(\boldsymbol{\eta}, \boldsymbol{\zeta})}{\partial \eta_{d_\eta} \partial \zeta_{d_\zeta}} \end{bmatrix}.$$

We suppress $\nabla_{\boldsymbol{\eta}} \nabla_{\boldsymbol{\eta}}$ to $\nabla_{\boldsymbol{\eta}}^2$. Note that $\nabla_{\boldsymbol{\eta}, \boldsymbol{\zeta}}^2 g(\boldsymbol{\eta}, \boldsymbol{\zeta})$ is the Hessian of $g(\boldsymbol{\eta}, \boldsymbol{\zeta})$.

Consider $p \in \mathbb{N}_1$ and a sequence indexed by two subscripts $\{x_{st}\}$ where $1 \leq s < t \leq p$. Whenever we write $x_{12}, \dots, x_{(p-1)p}$, we mean

$$x_{12}, \dots, x_{1p}, x_{23}, \dots, x_{2p}, \dots, x_{(p-2)(p-1)}, x_{(p-2)p}, x_{(p-1)p}$$

where the elements are ordered in a row-major manner.

2.2 Multivariate Latent Gaussian Model

Suppose $p \in \mathbb{N}_1$, $n \in \mathbb{N}_1$ and $\mathbf{y}_1, \dots, \mathbf{y}_n$ are i.i.d. p -dimensional observations from some multivariate latent Gaussian model. Letting $\mathbf{y} = (y_1, \dots, y_p)^\top \in$

$\mathcal{Y} \subseteq \mathbb{R}^p$ and introducing $\mathbf{x} = (x_1, \dots, x_p)^\top \in \mathbb{R}^p$, the density function of the model can be written as

$$f(\mathbf{y}|\boldsymbol{\mu}, \boldsymbol{\Sigma}) = \int \prod_{j=1}^p h_j(y_j|x_j)\phi(\mathbf{x}|\boldsymbol{\mu}, \boldsymbol{\Sigma})d\mathbf{x}, \quad (1)$$

where h_j 's are univariate density functions, $\boldsymbol{\Sigma} = \{\sigma_{st}\}$ is a $p \times p$ positive definite matrix and $\boldsymbol{\mu} = (\mu_1, \dots, \mu_p)^\top \in \mathbb{R}^p$. We refer to h_j 's as link densities.

The integral in (1) usually does not have an analytical solution, and accurate numerical integration is infeasible even for moderately large p . Hence, fully Bayesian inference is usually based on a DA-MCMC algorithm, where \mathbf{x} is augmented and sampled together with the model parameters $\boldsymbol{\mu}$ and $\boldsymbol{\Sigma}$.

If we let h_j 's be discrete data densities, then (1) provides a rich class of multivariate discrete data models. However, real world discrete datasets are often severely imbalanced. Taking online advertising as an example, the click through rate of a certain link is usually very close to 0. Supposing that one wants to fit a logistic regression to predict the probability of a certain user's clicking the link, only a tiny fraction of the responses will be 1.

Unfortunately, DA-MCMC has a provably slow mixing rate in imbalanced discrete data problems. Considering an intercept-only probit model and assuming that the data are infinite imbalanced, Johndrow et al. [2016] have shown that the step size of DA-MCMC is roughly $O(\frac{1}{\sqrt{n}})$, while the width of the high probability region of the posterior is roughly $O(\frac{1}{\log n})$. For large n , the step size will become much smaller than the width of the high probability bulk, causing extreme slow mixing. Moreover, this mismatch will become worse as n grows, and presents huge practical problems in broad settings.

Another drawback of DA-MCMC is its poor scalability to large sample size. The per-iteration computational complexity is at least $O(n)$ due to the need to sample an augmented \mathbf{x}_i for each \mathbf{y}_i . Moreover, the number of model parameters in (1) increases quadratically as the data dimensionality grows.

One way to bypass DA-MCMC is to evaluate the integral in (1) directly via deterministic numerical integration methods. Unfortunately, these methods are only feasible for small p . A potential solution is to approximate Bayesian inference by using a composite likelihood whose individual components are low-dimensional conditional or marginal densities that can be numerically evaluated [Pauli et al., 2011]. *Bayesian mosaic* is partially motivated by this idea.

Suppose $\mathbf{y} = (y_1, \dots, y_p)^\top$ follows the multivariate latent Gaussian model whose density function is defined in (1). One can easily prove the following:

i) For $j = 1, \dots, p$, the univariate marginal density for y_j is

$$f_{jj}(y_j|\mu_j, \sigma_{jj}) = \int h_j(y_j|x_j)\phi(x_j|\mu_j, \sigma_{jj})dx_j,$$

ii) For $1 \leq s < t \leq p$, the bivariate marginal density for y_s and y_t is

$$\begin{aligned} & f_{st}(y_s, y_t|\sigma_{st}, \mu_s, \sigma_{ss}, \mu_t, \sigma_{tt}) \\ &= \int h_s(y_s|x_1)h_t(y_t|x_2)\phi\left(\begin{bmatrix} x_1 \\ x_2 \end{bmatrix} \middle| \begin{bmatrix} \mu_s \\ \mu_t \end{bmatrix}, \begin{bmatrix} \sigma_{ss} & \sigma_{st} \\ \sigma_{ts} & \sigma_{tt} \end{bmatrix}\right)d\begin{bmatrix} x_1 \\ x_2 \end{bmatrix}. \end{aligned}$$

There is a rich literature on numerical integration methods for univariate and bivariate functions. Hence f_{jj} 's and f_{st} 's can be efficiently evaluated. In fact, many composite likelihood methods have been using these lower-dimensional densities as individual components due to the fact that they are computationally easier to work with [Cox and Reid, 2004].

Consider the following composite log-likelihood which consists of only univariate marginal densities:

$$Q_n(\boldsymbol{\mu}, \sigma_{11}, \dots, \sigma_{pp}) = \sum_i^n \sum_{j=1}^p \ell_{jj}(y_{ij}|\mu_j, \sigma_{jj}),$$

where $\ell_{jj}(y_j|\mu_j, \sigma_{jj}) = \log f_{jj}(y_j|\mu_j, \sigma_{jj})$ for $j = 1, \dots, p$. One can construct the following posterior distribution:

$$\pi_n^*(\boldsymbol{\mu}, \sigma_{11}, \dots, \sigma_{pp}) \propto \exp\{Q_n(\boldsymbol{\mu}, \sigma_{11}, \dots, \sigma_{pp})\} \pi(\boldsymbol{\mu}, \sigma_{11}, \dots, \sigma_{pp}),$$

given prior $\pi(\boldsymbol{\mu}, \sigma_{11}, \dots, \sigma_{pp})$. If we assume prior independence, so that $\pi(\boldsymbol{\mu}, \sigma_{11}, \dots, \sigma_{pp}) = \prod_{j=1}^p \pi_{jj}(\mu_j, \sigma_{jj})$, and let

$$\pi_{n,jj}^*(\mu_j, \sigma_{jj}) \propto \exp\left\{\sum_i^n \ell_{jj}(y_{ij}|\mu_j, \sigma_{jj})\right\} \pi_{jj}(\mu_j, \sigma_{jj}),$$

it can be shown that

$$\pi_n^*(\boldsymbol{\mu}, \sigma_{11}, \dots, \sigma_{pp}) = \prod_{j=1}^p \pi_{n,jj}^*(\mu_j, \sigma_{jj}). \quad (2)$$

We have constructed a surrogate posterior distribution for $\boldsymbol{\mu}$ and σ_{jj} 's. These are the parameters that characterize the univariate marginal distributions of the data. The factorized form of the composite likelihood and prior independence induces posterior independence in (μ_j, σ_{jj}) 's. Therefore, sampling from (2) can be split into independently sampling from each $\pi_{n,jj}^*(\mu_j, \sigma_{jj})$.

To complete our surrogate posterior distribution, we need some conditional distribution of σ_{st} 's given $\boldsymbol{\mu}$ and σ_{jj} 's. Consider the following composite log-likelihood:

$$L_n(\boldsymbol{\mu}, \boldsymbol{\Sigma}) = \sum_i^n \sum_{s < t}^p \ell_{st}(y_{is}, y_{it} | \sigma_{st}, \mu_s, \sigma_{ss}, \mu_t, \sigma_{tt}),$$

where $\ell_{st}(y_s, y_t | \sigma_{st}, \mu_s, \sigma_{ss}, \mu_t, \sigma_{tt}) = \log f_{st}(y_s, y_t | \sigma_{st}, \mu_s, \sigma_{ss}, \mu_t, \sigma_{tt})$ for $1 \leq s < t \leq p$. This time we will assume prior conditional independence, i.e., the prior density takes the following factorized form:

$$\pi(\sigma_{12}, \dots, \sigma_{(p-1)p} | \boldsymbol{\mu}, \sigma_{11}, \dots, \sigma_{pp}) = \prod_{1 \leq s < t \leq p}^p \pi_{st}(\sigma_{st} | \mu_s, \sigma_{ss}, \mu_t, \sigma_{tt}).$$

Letting

$$\begin{aligned} & \pi_{n,st}^*(\sigma_{st} | \mu_s, \sigma_{ss}, \mu_t, \sigma_{tt}) \\ & \propto \exp \left\{ \sum_i^n \ell_{st}(y_{is}, y_{it} | \sigma_{st}, \mu_s, \sigma_{ss}, \mu_t, \sigma_{tt}) \right\} \pi_{st}(\sigma_{st} | \mu_s, \sigma_{ss}, \mu_t, \sigma_{tt}), \end{aligned}$$

we can construct the following conditional posterior density:

$$\pi_n^*(\sigma_{12}, \dots, \sigma_{(p-1)p} | \boldsymbol{\mu}, \sigma_{11}, \dots, \sigma_{pp}) = \prod_{1 \leq s < t \leq p}^p \pi_{n,st}^*(\sigma_{st} | \mu_s, \sigma_{ss}, \mu_t, \sigma_{tt}). \quad (3)$$

Similarly, we have posterior conditional independence in σ_{st} 's given $\boldsymbol{\mu}$ and σ_{jj} 's. Therefore, sampling from (3) can be split into independently sampling from each $\pi_{n,st}^*(\sigma_{st} | \mu_s, \sigma_{ss}, \mu_t, \sigma_{tt})$.

Combining (2) and (3) we construct the following surrogate posterior density:

$$\pi_n^*(\boldsymbol{\mu}, \boldsymbol{\Sigma}) = \pi_n^*(\sigma_{12}, \dots, \sigma_{(p-1)p} | \boldsymbol{\mu}, \sigma_{11}, \dots, \sigma_{pp}) \pi_n^*(\boldsymbol{\mu}, \sigma_{11}, \dots, \sigma_{pp}).$$

To summarize, we have proposed a surrogate posterior distribution which is a multiplication of component posteriors. These component posteriors are based on either univariate or bivariate marginal densities. Sampling from this posterior can be done via a composite sampling strategy that contains two steps. In the first step, we sample the parameters that characterize the univariate marginal densities ($\boldsymbol{\mu}$ and σ_{jj} 's). In the second step, we plug the previous samples into the conditional densities and sample those parameters that characterize the pairwise relationship (σ_{st} 's). The computation of both steps can be easily parallelized due to the sparse posterior dependence structure. We term $\pi_n^*(\boldsymbol{\mu}, \boldsymbol{\Sigma})$ as a *Bayesian mosaic* posterior under model (1). A formal definition will follow.

2.3 Definition of Bayesian Mosaic

It can be seen that the independence structure in (2) relies on the fact that univariate marginal distributions do not share parameters, and that the conditional independence structure in (3) requires that the parameters characterizing the pairwise relationships (σ_{st} 's) only appear in one bivariate marginal distribution. We term the class of data distributions that satisfy the above conditions as *mosaic-type*. Below is a formal definition.

Definition 2.1. Suppose $p \in \mathbb{N}_1$ and $\mathbf{y}_1, \dots, \mathbf{y}_n$ are i.i.d. p -dimensional data vectors from distribution $P_{\boldsymbol{\theta}}$ with density function $f(\mathbf{y}|\boldsymbol{\theta})$. Let $\boldsymbol{\theta}_{st}$, $1 \leq s \leq t \leq p$, be non-overlapping sub-vectors of $\boldsymbol{\theta}$ such that

$$\boldsymbol{\theta} = [\boldsymbol{\theta}_{12}^\top, \dots, \boldsymbol{\theta}_{(p-1)p}^\top, \boldsymbol{\theta}_{11}^\top, \dots, \boldsymbol{\theta}_{pp}^\top]^\top,$$

then the data distribution $P_{\boldsymbol{\theta}}$ is *mosaic-type* if there exists a collection of density functions f_{st} for $1 \leq s \leq t \leq p$ such that

- i) for $j = 1, \dots, p$, the density of the univariate marginal distribution for dimension j is

$$f_{jj}(y_j|\boldsymbol{\theta}_{jj}).$$

- ii) for $1 \leq t < s \leq p$, the density of the bivariate marginal data distribution for dimension s and t is

$$f_{st}(y_s, y_t|\boldsymbol{\theta}_{st}, \boldsymbol{\theta}_{ss}, \boldsymbol{\theta}_{tt}).$$

We term $\boldsymbol{\theta}_{jj}$'s as *knots* since they are shared among multiple bivariate marginal distributions. We term $\boldsymbol{\theta}_{st}$'s as *tiles* since they only appear in one bivariate marginal distribution. In the multivariate latent Gaussian example,

$$\boldsymbol{\theta}_{jj} = \begin{bmatrix} \mu_j \\ \sigma_{jj} \end{bmatrix}, \quad \boldsymbol{\theta}_{st} = \sigma_{st}.$$

We will show that Definition 2.1 provides a rich class of models later in §3.1. Although we require $\mathbf{y}_1, \dots, \mathbf{y}_n$ to be independent for now, to ease our analysis of asymptotic properties, in practice this requirement can be relaxed. We provide a more general definition in §2.6.

Before defining *Bayesian mosaic*, we will first introduce some notation. For $j = 1, \dots, p$, define

$$\ell_{jj}(\boldsymbol{\theta}_{jj}, y_j) = \log f_{jj}(y_j | \boldsymbol{\theta}_{jj}), \quad Q_{n,j}(\boldsymbol{\theta}_{jj}) = \sum_{i=1}^n \ell_{jj}(\boldsymbol{\theta}_{jj}, y_{ij}).$$

For $1 \leq s < t \leq p$, define

$$\begin{aligned} \ell_{st}(\boldsymbol{\theta}_{st}, \boldsymbol{\theta}_{ss}, \boldsymbol{\theta}_{tt}, y_s, y_t) &= \log f_{st}(y_s, y_t | \boldsymbol{\theta}_{st}, \boldsymbol{\theta}_{ss}, \boldsymbol{\theta}_{tt}), \\ L_{n,st}(\boldsymbol{\theta}_{st}, \boldsymbol{\theta}_{ss}, \boldsymbol{\theta}_{tt}) &= \sum_{i=1}^n \ell_{st}(\boldsymbol{\theta}_{st}, \boldsymbol{\theta}_{ss}, \boldsymbol{\theta}_{tt}, y_{is}, y_{it}). \end{aligned}$$

The formal definition of *Bayesian mosaic* is given below.

Definition 2.2. *Under the setup of Definition 2.1 and considering prior densities $\pi_{jj}(\boldsymbol{\theta}_{jj})$ for $j = 1, \dots, p$ and $\pi_{st}(\boldsymbol{\theta}_{st} | \boldsymbol{\theta}_{ss}, \boldsymbol{\theta}_{tt})$ for $1 \leq t < s \leq p$, we introduce the following:*

i) For $j = 1, \dots, p$, the knot marginal for $\boldsymbol{\theta}_{jj}$ is

$$\kappa_{n,j}(\boldsymbol{\theta}_{jj}) \propto e^{Q_{n,j}(\boldsymbol{\theta}_{jj})} \pi_{jj}(\boldsymbol{\theta}_{jj}).$$

ii) For $1 \leq t < s \leq p$, the tile conditional for $\boldsymbol{\theta}_{st}$ given $\boldsymbol{\theta}_{ss}$ and $\boldsymbol{\theta}_{tt}$ is

$$\tau_{n,st}(\boldsymbol{\theta}_{st} | \boldsymbol{\theta}_{ss}, \boldsymbol{\theta}_{tt}) \propto e^{L_{n,st}(\boldsymbol{\theta}_{st}, \boldsymbol{\theta}_{ss}, \boldsymbol{\theta}_{tt})} \pi_{st}(\boldsymbol{\theta}_{st} | \boldsymbol{\theta}_{ss}, \boldsymbol{\theta}_{tt}).$$

Then we call

$$\tilde{\pi}(\boldsymbol{\theta}) = \prod_j^p \kappa_{n,j}(\boldsymbol{\theta}_{jj}) \prod_{s < t}^p \tau_{n,st}(\boldsymbol{\theta}_{st} | \boldsymbol{\theta}_{ss}, \boldsymbol{\theta}_{tt}) \quad (4)$$

a *Bayesian mosaic posterior* under model $P_{\boldsymbol{\theta}}$.

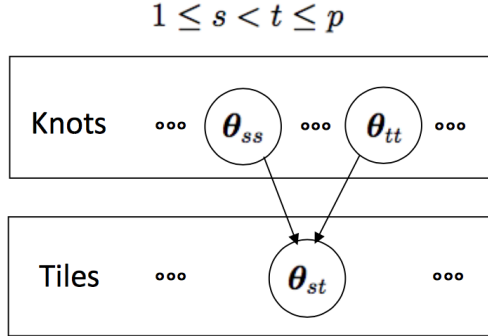


Figure 1: DAG representation of a *Bayesian mosaic*.

2.4 Sampling Bayesian Mosaic

It is easily seen from (4) that the *knots* are marginally independent and the *tiles* are conditionally independent given the *knots*. This sparse dependence structure of *Bayesian mosaic* can be represented by a directed acyclic graph (DAG), as demonstrated in Figure 1. Utilizing this structure, we propose a simple parallel sampling strategy which is summarized in Algorithm 1, where $M \in \mathbb{N}_1$ denotes the total number of posterior samples to be collected.

```

Step 1 # on each of the knot marginals in parallel
for  $j = 1, \dots, p$  do
  | sample  $\theta_{jj}^1, \dots, \theta_{jj}^M$  from  $\kappa_{n,j}(\theta_{jj})$ 
end
Step 2 # on each of the tile conditionals in parallel
for  $s = 2, \dots, p$  do
  | for  $t = 1, \dots, s - 1$  do
  | | sample  $\theta_{st}^m$  from  $\tau_{n,st}(\theta_{st} | \theta_{ss}^m, \theta_{tt}^m)$ , for  $m = 1, \dots, M$ 
  | end
end

```

Algorithm 1: Parallel sampler for *Bayesian mosaic*.

Usually, the *knot marginals* and the *tile conditionals* can not be directly sampled from. We propose to sample the *knot marginals* via Metropolis-Hastings (MH) algorithms with the $Q_n(\theta_{jj})$'s being evaluated via numerical integration. Sampling from the *tile conditionals* is harder, since the condi-

tional distribution $\tau_{n,st}(\boldsymbol{\theta}_{st}|\boldsymbol{\theta}_{ss}^m, \boldsymbol{\theta}_{tt}^m)$ changes w.r.t. the values of $\boldsymbol{\theta}_{ss}^m$ and $\boldsymbol{\theta}_{tt}^m$. We propose the following three options:

- i) Suppose that the MH sampler on $\tau_{n,st}(\boldsymbol{\theta}_{st}|\boldsymbol{\theta}_{ss}^m, \boldsymbol{\theta}_{tt}^m)$ converges rapidly, then for each m , one can run the sampler for a fixed small number of steps and use the last draw as the sample.
- ii) Suppose that $\tau_{n,st}(\boldsymbol{\theta}_{st}|\boldsymbol{\theta}_{ss}^m, \boldsymbol{\theta}_{tt}^m)$ is easy to optimize w.r.t. $\boldsymbol{\theta}_{st}$, then one can compute the mode and the maximum density value. Then one can either do rejection sampling using the maximum density value or obtain the Hessian matrix at the mode and approximate the density by its Laplace approximation.
- iii) One can directly plug in the posterior means of the *knots* into the *tile conditionals* so that they remain the same across iterations. Simply substitute $\tau_{n,st}(\boldsymbol{\theta}_{st}|\boldsymbol{\theta}_{ss}^m, \boldsymbol{\theta}_{tt}^m)$ in the second step of Algorithm 1 with $\tau_{n,st}\left(\boldsymbol{\theta}_{st} \mid \frac{1}{M} \sum_{m=1}^M \boldsymbol{\theta}_{ss}^m, \frac{1}{M} \sum_{m=1}^M \boldsymbol{\theta}_{tt}^m\right)$.

The third option is the fallback plan when the first two are unavailable. Note that when applying the third option, instead of sampling from the *Bayesian mosaic*, one actually samples from the following approximation:

$$\prod_j^p \kappa_{n,j}(\boldsymbol{\theta}_{jj}) \prod_{s<t}^p \tau_{n,st}(\boldsymbol{\theta}_{st}|\boldsymbol{\theta}_{ss}^*, \boldsymbol{\theta}_{tt}^*), \quad (5)$$

where $\boldsymbol{\theta}_{jj}^* = \int \kappa_{n,j}(\boldsymbol{\theta}_{jj})d\boldsymbol{\theta}_{jj}$ is the posterior mean of $\boldsymbol{\theta}_{jj}$, for $j = 1, \dots, p$. In §3.3 we will show that (5) is still consistent and asymptotically normal in a slightly weaker sense, but will underestimate the uncertainty compared to the exact *Bayesian mosaic*.

2.5 Handling Parameter Constraints

In some cases, the model parameters $\boldsymbol{\theta}$ live in a constrained space \mathcal{T} . However, the samples from *Bayesian mosaic* do not necessarily also live in this space. For instance, in (1), the samples of $\boldsymbol{\Sigma}$ from *Bayesian mosaic* are not guaranteed to be positive definite. One can easily see this from the fact that the off-diagonal elements σ_{st} 's are conditionally independent given the diagonal elements σ_{jj} 's.

To address this, we propose to project the samples from *Bayesian mosaic* back to the constrained space w.r.t. the Euclidean distance. Specifically, we solve the following optimization problem for each sample $\boldsymbol{\theta}^m$:

$$\tilde{\boldsymbol{\theta}}^m = \arg \min_{\boldsymbol{\theta}^m \in \mathcal{T}} \|\tilde{\boldsymbol{\theta}}^m - \boldsymbol{\theta}^m\|. \quad (6)$$

We term $\tilde{\boldsymbol{\theta}}^m$'s as the corrected samples from *Bayesian mosaic*. For many structured constrained parameter spaces \mathcal{T} , (6) has an analytical solution. For instance, if \mathcal{T} is the cone of positive definite matrices, then $\tilde{\boldsymbol{\theta}}^m$ can be obtained via an eigenvalue decomposition of $\boldsymbol{\theta}^m$.

In §3.2, we will prove that the probability mass of *Bayesian mosaic* asymptotically concentrates within a small neighbourhood of the “true” value $\boldsymbol{\theta}_0$. This implies that when n is large for many constraints, the majority of the samples should automatically live inside \mathcal{T} and we only need to correct the rest. Hence, this correcting step should have minimal impact on the overall performance.

2.6 Generalization

In this subsection, we will extend *Bayesian mosaic* to dependent data. We first provide a more general definition of *mosaic-type* data distributions.

Definition 2.3. Suppose $p \in \mathbb{N}_1$ and $\mathbf{y}_1, \dots, \mathbf{y}_n$ are p -dimensional data vectors jointly from distribution $P_{\boldsymbol{\theta}}$ with a joint density function $f(\mathbf{y}_1, \dots, \mathbf{y}_n | \boldsymbol{\theta})$. Let $\boldsymbol{\theta}_{st}$, $1 \leq t \leq s \leq p$, be non-overlapping sub-vectors of $\boldsymbol{\theta}$ such that

$$\boldsymbol{\theta} = [\boldsymbol{\theta}_{12}^\top, \dots, \boldsymbol{\theta}_{(p-1)p}^\top, \boldsymbol{\theta}_{11}^\top, \dots, \boldsymbol{\theta}_{pp}^\top]^\top,$$

then the data distribution $P_{\boldsymbol{\theta}}$ is *mosaic-type* if there exists a collection of density functions f_{st} , $1 \leq s \leq t \leq p$ such that

- i) for $j = 1, \dots, p$, the density of the univariate marginal distribution for dimension j is

$$f_{jj}(y_{1j}, \dots, y_{nj} | \boldsymbol{\theta}_{jj}).$$

- ii) for $1 \leq t < s \leq p$, the density of the bivariate marginal data distribution for dimension s and t is

$$f_{st}(y_{1s}, \dots, y_{ns}, y_{1t}, \dots, y_{nt} | \boldsymbol{\theta}_{st}, \boldsymbol{\theta}_{ss}, \boldsymbol{\theta}_{tt}).$$

For $j = 1, \dots, p$, we redefine $Q_{n,j}(\boldsymbol{\theta}_{jj})$ as

$$Q_{n,j}(\boldsymbol{\theta}_{jj}) = \log f_{jj}(y_{1j}, \dots, y_{nj} | \boldsymbol{\theta}_{jj}).$$

For $1 \leq s < t \leq p$, we redefine $L_{n,st}(\boldsymbol{\theta}_{st}, \boldsymbol{\theta}_{ss}, \boldsymbol{\theta}_{tt})$ as

$$L_{n,st}(\boldsymbol{\theta}_{st}, \boldsymbol{\theta}_{ss}, \boldsymbol{\theta}_{tt}) = \log f_{st}(y_{1s}, \dots, y_{ns}, y_{1t}, \dots, y_{nt} | \boldsymbol{\theta}_{st}, \boldsymbol{\theta}_{ss}, \boldsymbol{\theta}_{tt}).$$

Then *Bayesian mosaic* still follows Definition 2.2.

Under this generalization, one can include random effects and still be able to use *Bayesian mosaic*. We will give an example of such a model in §4.3, where we include random temporal effects.

3 Theoretical Analysis

In this section we will first demonstrate that the *mosaic-type* class contains a rich collection of models. We will then provide regularity conditions and prove under these conditions that *Bayesian mosaic* is consistent and asymptotically normal. Moreover, we will analyze the asymptotic distribution of the *tiles* conditional on the posterior means of the *knots*. Finally we will build a connection between the sampling computational complexity and the cardinality of the data. We prove the main result and defer other proofs to the supplement.

3.1 Richness of the Mosaic-type Distribution Class

To evaluate how widely *Bayesian mosaic* can be applied in practice, it is crucial to understand how rich the *mosaic-type* distribution class is. The following lemma provides one simple rule to construct new *mosaic-type* distributions from any existing *mosaic-type* distributions. With the help of this rule, one can build models for any type of data with the dependence induced by latent variables with some underlying *mosaic-type* distribution.

Lemma 3.1. *Suppose that P_ψ is some data distribution with density function $f_0(\mathbf{x}|\psi)$ and consider another data distribution $P_{\boldsymbol{\mu},\psi}$ with the following density function:*

$$f(\mathbf{y}|\boldsymbol{\mu}, \psi) = \int f_0(\mathbf{x}|\psi) \prod_{j=1}^p g_j(y_j|x_j, \boldsymbol{\mu}_j) d\mathbf{x}, \quad (7)$$

where $\boldsymbol{\mu} = (\boldsymbol{\mu}_1^\top, \dots, \boldsymbol{\mu}_p^\top)^\top$ and g_j 's are proper density functions. If P_ψ is mosaic-type, so is $P_{\boldsymbol{\mu}, \psi}$.

One could choose P_ψ to be the multivariate Gaussian distribution, and $g_j(y_j|x_j, \boldsymbol{\mu}_j)$'s to be any univariate density. This implies that the *mosaic-type* model class contains the multivariate latent Gaussian models. Note that besides Gaussian, P_ψ could also be a Dirichlet or a multinomial distribution. It is easy to check that both distributions are *mosaic-type*. Moreover, one can construct arbitrarily complex models by repeatedly applying Lemma 3.1.

3.2 Posterior Consistency & Asymptotic Normality

We start our analysis in a simpler yet more general setup. Consider $p \in \mathbb{N}_1$, $d \in \mathbb{N}_1$ and $\mathbf{y}_1, \dots, \mathbf{y}_n$ which are i.i.d. p -dimensional observations from distribution P_θ possessing a density $f(\mathbf{y}|\theta)$ where $\theta \in \mathcal{T} \subset \mathbb{R}^d$. We fix θ_0 to be the ‘‘true value’’ of the parameters and require that θ_0 is an interior point of \mathcal{T} . Consider two non-overlapping sub-vectors of θ , $\boldsymbol{\eta}$ and $\boldsymbol{\zeta}$, where $\boldsymbol{\eta}$ is d_η -dimensional and $\boldsymbol{\zeta}$ is d_ζ -dimensional. Let $\boldsymbol{\eta}_0$ and $\boldsymbol{\zeta}_0$ be the corresponding ‘‘true values’’. Consider two pseudo density functions $f_1(\mathbf{y}|\boldsymbol{\zeta})$ and $f_2(\mathbf{y}|\boldsymbol{\eta}, \boldsymbol{\zeta})$, which do not have to integrate to one. In order for proper Bayesian inference, the following regularity conditions need to hold for both functions. To avoid redundancy, we only define these conditions for $f_1(\mathbf{y}|\boldsymbol{\zeta})$.

Condition 1. *The support set $\{\mathbf{y} : f_1(\mathbf{y}|\boldsymbol{\zeta}) > 0\}$ is the same for all $\boldsymbol{\zeta}$.*

Condition 2. *Consider $\ell_1(\boldsymbol{\zeta}, \mathbf{y}) = \log f_1(\mathbf{y}|\boldsymbol{\zeta})$. $\ell_1(\boldsymbol{\zeta}, \mathbf{y})$ is thrice differentiable with respect to $\boldsymbol{\zeta}$ in a neighborhood $\mathcal{B}_\zeta(\boldsymbol{\zeta}_0, \delta)$. The expectations $\mathbb{E}_{\theta_0} \nabla_\zeta \ell_1(\boldsymbol{\zeta}, \mathbf{y})$ and $\mathbb{E}_{\theta_0} \nabla_\zeta^2 \ell_1(\boldsymbol{\zeta}, \mathbf{y})$ are both finite and for any multi-index $\boldsymbol{\alpha}$ for $\boldsymbol{\zeta}$ such that $|\boldsymbol{\alpha}| = 3$, we have*

$$\sup_{\boldsymbol{\zeta} \in \mathcal{B}_\zeta(\boldsymbol{\zeta}_0, \delta)} |\partial^\alpha \ell_1(\boldsymbol{\zeta}, \mathbf{y})| \leq M_\alpha(\mathbf{y}),$$

and $\mathbb{E}_{\theta_0} M_\alpha(\mathbf{y}) < \infty$.

Condition 3. *Consider $\ell_1(\boldsymbol{\zeta}, \mathbf{y}) = \log f_1(\mathbf{y}|\boldsymbol{\zeta})$. Then $\mathbb{E}_{\theta_0} \nabla_\zeta \ell_1(\boldsymbol{\zeta}, \mathbf{y})|_{\boldsymbol{\zeta}=\boldsymbol{\zeta}_0} = \mathbf{0}$ and*

$$\mathbb{E}_{\theta_0} \nabla_\zeta^2 \ell_1(\boldsymbol{\zeta}, \mathbf{y})|_{\boldsymbol{\zeta}=\boldsymbol{\zeta}_0} = -\mathbb{E}_{\theta_0} [\nabla_\zeta \ell_1(\boldsymbol{\zeta}, \mathbf{y})] [\nabla_\zeta \ell_1(\boldsymbol{\zeta}, \mathbf{y})]^\top |_{\boldsymbol{\zeta}=\boldsymbol{\zeta}_0}$$

Also, the Fisher information $-\mathbb{E}_{\theta_0} \nabla_\zeta^2 \ell_1(\boldsymbol{\zeta}, \mathbf{y})|_{\boldsymbol{\zeta}=\boldsymbol{\zeta}_0}$ is positive definite.

Condition 4. Consider $Q_n(\boldsymbol{\zeta}) = \sum_{i=1}^n \log f_1(\mathbf{y}_i|\boldsymbol{\zeta})$. For any $\delta > 0$, $\exists \epsilon > 0$ such that with $P_{\boldsymbol{\theta}_0}$ -probability one

$$\sup_{\boldsymbol{\zeta} \notin \mathcal{B}_{\boldsymbol{\zeta}_0, \delta}} \frac{1}{n} [Q_n(\boldsymbol{\zeta}) - Q_n(\boldsymbol{\zeta}_0)] < -\epsilon$$

for all sufficiently large n .

Condition 5. Consider $Q_n(\boldsymbol{\zeta}) = \sum_{i=1}^n \log f_1(\mathbf{y}_i|\boldsymbol{\zeta})$ and $\tilde{\boldsymbol{\zeta}}_n = \arg \max_{\boldsymbol{\zeta}} Q_n(\boldsymbol{\zeta})$. $\tilde{\boldsymbol{\zeta}}_n$ is consistent at $\boldsymbol{\zeta}_0$, i.e., $\lim_{n \rightarrow \infty} \tilde{\boldsymbol{\zeta}}_n = \boldsymbol{\zeta}_0$ with $P_{\boldsymbol{\theta}_0}$ -probability one.

For ease of presentation, we introduce some notation. We define

$$\begin{aligned} \ell_1(\boldsymbol{\zeta}, \mathbf{y}) &= \log f_1(\mathbf{y}|\boldsymbol{\zeta}), & Q_n(\boldsymbol{\zeta}) &= \sum_{i=1}^n \ell_1(\boldsymbol{\zeta}, \mathbf{y}_i), \\ \ell_2(\boldsymbol{\eta}, \boldsymbol{\zeta}, \mathbf{y}) &= \log f_2(\mathbf{y}|\boldsymbol{\eta}, \boldsymbol{\zeta}), & L_n(\boldsymbol{\eta}, \boldsymbol{\zeta}) &= \sum_{i=1}^n \ell_2(\boldsymbol{\eta}, \boldsymbol{\zeta}, \mathbf{y}_i), \\ [\hat{\boldsymbol{\eta}}_n] &= \arg \max_{\boldsymbol{\eta}, \boldsymbol{\zeta}} L_n(\boldsymbol{\eta}, \boldsymbol{\zeta}), & \tilde{\boldsymbol{\zeta}}_n &= \arg \max_{\boldsymbol{\zeta}} Q_n(\boldsymbol{\zeta}), \end{aligned}$$

and

$$\tilde{\mathbf{I}}_0 = -\mathbb{E}_{\boldsymbol{\theta}_0} \nabla_{\boldsymbol{\zeta}}^2 \ell_1(\boldsymbol{\zeta}, \mathbf{y})|_{\boldsymbol{\theta}=\boldsymbol{\theta}_0}, \quad \mathbf{I}_0 = -\mathbb{E}_{\boldsymbol{\theta}_0} \nabla_{\boldsymbol{\eta}, \boldsymbol{\zeta}}^2 \ell_2(\boldsymbol{\eta}, \boldsymbol{\zeta}, \mathbf{y})|_{\boldsymbol{\theta}=\boldsymbol{\theta}_0}.$$

Given a prior density $\pi(\boldsymbol{\zeta})$, consider the following posterior density of $\boldsymbol{\zeta}$:

$$\kappa_n(\boldsymbol{\zeta}) \propto \exp\{Q_n(\boldsymbol{\zeta})\} \pi(\boldsymbol{\zeta}).$$

Introducing $\boldsymbol{\omega} = \sqrt{n}(\boldsymbol{\zeta} - \tilde{\boldsymbol{\zeta}}_n)$, the posterior density of $\boldsymbol{\omega}$ is

$$\pi_{n,1}^*(\boldsymbol{\omega}) = \frac{1}{\sqrt{n}} \kappa_n \left(\frac{\boldsymbol{\omega}}{\sqrt{n}} + \tilde{\boldsymbol{\zeta}}_n \right).$$

The following lemmas state that $\pi_{n,1}^*(\boldsymbol{\omega})$ is asymptotically normal under the specified conditions. This lemma is basically the multivariate version of Theorem 4.2 in Ghosh et al. [2007], hence the proof will be omitted.

Lemma 3.2. Suppose that conditions 1-5 hold for $f_1(\mathbf{y}|\boldsymbol{\zeta})$, and the prior density $\pi(\boldsymbol{\zeta})$ is continuous and positive at $\boldsymbol{\zeta}_0$, then with $P_{\boldsymbol{\theta}_0}$ -probability one

$$\lim_{n \rightarrow \infty} \int |\pi_{n,1}^*(\boldsymbol{\omega}) - \phi(\boldsymbol{\omega}|\mathbf{0}, \tilde{\mathbf{I}}_0^{-1})| d\boldsymbol{\omega} = 0. \quad (8)$$

With a prior density $\pi(\boldsymbol{\eta}|\boldsymbol{\zeta})$, consider the following conditional posterior density of $\boldsymbol{\eta}$ given $\boldsymbol{\zeta}$:

$$\tau_n(\boldsymbol{\eta}|\boldsymbol{\zeta}) \propto \exp \{L_n(\boldsymbol{\eta}, \boldsymbol{\zeta}) - L_n(\hat{\boldsymbol{\eta}}_n, \hat{\boldsymbol{\zeta}}_n)\} \pi(\boldsymbol{\eta}|\boldsymbol{\zeta}).$$

Introducing $\mathbf{t} = \sqrt{n}(\boldsymbol{\eta} - \hat{\boldsymbol{\eta}}_n)$ and $\mathbf{r} = \sqrt{n}(\boldsymbol{\zeta} - \hat{\boldsymbol{\zeta}}_n)$, the conditional posterior density of \mathbf{t} given \mathbf{r} can be written as

$$\begin{aligned} \pi_{n,2}^*(\mathbf{t}|\mathbf{r}) &= a_n^{-1}(\mathbf{r}) \exp \{L_n(\hat{\boldsymbol{\eta}}_n + \mathbf{t}/\sqrt{n}, \hat{\boldsymbol{\zeta}}_n + \mathbf{r}/\sqrt{n}) - L_n(\hat{\boldsymbol{\eta}}_n, \hat{\boldsymbol{\zeta}}_n)\} \\ &\quad \times \pi(\hat{\boldsymbol{\eta}}_n + \mathbf{t}/\sqrt{n} | \hat{\boldsymbol{\zeta}}_n + \mathbf{r}/\sqrt{n}) \end{aligned}$$

with $a_n(\mathbf{r})$ being the normalizing constant. We define

$$\begin{aligned} \mathbf{I}_0^{11} &= -\mathbb{E}_{\boldsymbol{\theta}_0} \nabla_{\boldsymbol{\eta}}^2 \ell_2(\boldsymbol{\eta}, \boldsymbol{\zeta}, \mathbf{y}) |_{\boldsymbol{\theta}=\boldsymbol{\theta}_0}, & \mathbf{I}_0^{12} &= -\mathbb{E}_{\boldsymbol{\theta}_0} \nabla_{\boldsymbol{\zeta}} \nabla_{\boldsymbol{\eta}} \ell_2(\boldsymbol{\eta}, \boldsymbol{\zeta}, \mathbf{y}) |_{\boldsymbol{\theta}=\boldsymbol{\theta}_0}, \\ \mathbf{I}_0^{21} &= -\mathbb{E}_{\boldsymbol{\theta}_0} \nabla_{\boldsymbol{\eta}} \nabla_{\boldsymbol{\zeta}} \ell_2(\boldsymbol{\eta}, \boldsymbol{\zeta}, \mathbf{y}) |_{\boldsymbol{\theta}=\boldsymbol{\theta}_0}, & \mathbf{I}_0^{22} &= -\mathbb{E}_{\boldsymbol{\theta}_0} \nabla_{\boldsymbol{\zeta}}^2 \ell_2(\boldsymbol{\eta}, \boldsymbol{\zeta}, \mathbf{y}) |_{\boldsymbol{\theta}=\boldsymbol{\theta}_0}. \end{aligned}$$

It is easily seen that $\mathbf{I}_0 = \begin{bmatrix} \mathbf{I}_0^{11} & \mathbf{I}_0^{12} \\ \mathbf{I}_0^{21} & \mathbf{I}_0^{22} \end{bmatrix}$.

Theorem 3.3. *Suppose that the conditions for Lemma 3.2 hold, conditions 1-5 hold for $f_2(\mathbf{y}|\boldsymbol{\eta}, \boldsymbol{\zeta})$ and that the prior density $\pi(\boldsymbol{\eta}|\boldsymbol{\zeta})$ is continuous and positive at $\begin{bmatrix} \boldsymbol{\eta}_0 \\ \boldsymbol{\zeta}_0 \end{bmatrix}$, then with $P_{\boldsymbol{\theta}_0}$ -probability one*

$$\lim_{n \rightarrow \infty} \int \int \left| \pi_n^*(\mathbf{t}, \mathbf{r}) - \phi\left(\mathbf{t} \mid -(\mathbf{I}_0^{11})^{-1} \mathbf{I}_0^{12} \mathbf{r}, (\mathbf{I}_0^{11})^{-1}\right) \phi\left(\mathbf{r} \mid \boldsymbol{\mu}_n, \tilde{\mathbf{I}}_0^{-1}\right) \right| d\mathbf{r} d\mathbf{t} = 0, \quad (9)$$

where $\pi_n^*(\mathbf{t}, \mathbf{r}) = \pi_{n,2}^*(\mathbf{t}|\mathbf{r})\pi_{n,1}^*(\mathbf{r})$ is the joint posterior density of \mathbf{t} and \mathbf{r} and $\boldsymbol{\mu}_n = \sqrt{n}(\tilde{\boldsymbol{\zeta}}_n - \hat{\boldsymbol{\zeta}}_n)$.

Corollary 3.4. *Under the same setup in Theorem 3.3, $\tau_n(\boldsymbol{\eta}|\boldsymbol{\zeta}) \kappa_n(\boldsymbol{\zeta})$ is consistent at $\boldsymbol{\eta}_0$ and $\boldsymbol{\zeta}_0$.*

We can directly apply Theorem 3.3 and Corollary 3.4 to analyze the asymptotic properties of *Bayesian mosaic*. All we need is to let $f_1(\mathbf{y}|\boldsymbol{\zeta})$ be the multiplication of the densities of the univariate marginal distributions,

$$f_1(\mathbf{y}|\boldsymbol{\zeta}) = \prod_{j=1}^p f_{jj}(y_j|\boldsymbol{\theta}_{jj}),$$

$f_2(\mathbf{y}|\boldsymbol{\theta}, \boldsymbol{\zeta})$ be the multiplication of the densities of the bivariate marginal distributions,

$$f_2(\mathbf{y}|\boldsymbol{\theta}, \boldsymbol{\zeta}) = \prod_{1 \leq s < t \leq p} f_{st}(y_s, y_t | \boldsymbol{\theta}_{st}, \boldsymbol{\theta}_{ss}, \boldsymbol{\theta}_{tt}),$$

$\pi(\boldsymbol{\zeta})$ be the multiplication of the prior densities for *knots*,

$$\pi(\boldsymbol{\zeta}) = \prod_{j=1}^p \pi_{jj}(\boldsymbol{\theta}_{jj}),$$

and $\pi(\boldsymbol{\eta}|\boldsymbol{\zeta})$ be the multiplication of the conditional prior densities for *tiles*,

$$\pi(\boldsymbol{\eta}|\boldsymbol{\zeta}) = \prod_{1 \leq s < t \leq p} \pi_{st}(\boldsymbol{\theta}_{st} | \boldsymbol{\theta}_{ss}, \boldsymbol{\theta}_{tt}).$$

We immediately have

$$\ell_1(\boldsymbol{\zeta}, \mathbf{y}) = \sum_{j=1}^p \ell_{jj}(y_j | \boldsymbol{\theta}_{jj}), \quad \ell_2(\boldsymbol{\eta}, \boldsymbol{\zeta}, \mathbf{y}) = \sum_{1 \leq s < t \leq p} \ell_{st}(y_s, y_t | \boldsymbol{\theta}_{st}, \boldsymbol{\theta}_{ss}, \boldsymbol{\theta}_{tt}).$$

It can be shown that

$$\begin{aligned} \kappa_n(\boldsymbol{\zeta}) &\propto \exp \left\{ \sum_{i=1}^n \ell_1(\boldsymbol{\zeta}, \mathbf{y}_i) \right\} \pi(\boldsymbol{\zeta}) \\ &= \exp \left\{ \sum_{j=1}^p \sum_{i=1}^n \ell_{jj}(y_{ij} | \boldsymbol{\theta}_{jj}) \right\} \prod_{j=1}^p \pi_{jj}(\boldsymbol{\theta}_{jj}) \\ &= \prod_{j=1}^p \exp \left\{ \sum_{i=1}^n \ell_{jj}(y_{ij} | \boldsymbol{\theta}_{jj}) \right\} \pi_{jj}(\boldsymbol{\theta}_{jj}) \\ &= \prod_{j=1}^p \kappa_{n,jj}(\boldsymbol{\theta}_{jj}). \end{aligned}$$

Similarly we can show that

$$\tau_n(\boldsymbol{\eta}|\boldsymbol{\zeta}) = \prod_{s < t}^p \tau_{n,st}(\boldsymbol{\theta}_{st} | \boldsymbol{\theta}_{ss}, \boldsymbol{\theta}_{tt}).$$

Therefore $\tau_n(\boldsymbol{\eta}|\boldsymbol{\zeta})\kappa_n(\boldsymbol{\zeta})$ is exactly the *Bayesian mosaic*, specifically,

$$\tau_n(\boldsymbol{\eta}|\boldsymbol{\zeta})\kappa_n(\boldsymbol{\zeta}) = \prod_{s < t}^p \tau_{n,st}(\boldsymbol{\theta}_{st}|\boldsymbol{\theta}_{ss}, \boldsymbol{\theta}_{tt}) \prod_{j=1}^p \kappa_{n,jj}(\boldsymbol{\theta}_{jj}) = \tilde{\pi}_n(\boldsymbol{\theta}),$$

where $\boldsymbol{\theta} = \begin{bmatrix} \boldsymbol{\eta} \\ \boldsymbol{\zeta} \end{bmatrix}$. Consequently, Theorem 3.3 and Corollary 3.4 can be used directly to analyze the asymptotic properties of *Bayesian mosaic*. The following lemma provides sufficient conditions for the regularity conditions for Theorem 3.3 to hold. The proof of this lemma is straightforward and hence is omitted.

Lemma 3.5. *Suppose that for $j = 1, \dots, p$, $f_{jj}(\mathbf{y}|\boldsymbol{\eta}_{jj}) = f_{jj}(y_j|\boldsymbol{\eta}_{jj})$ satisfies conditions 1-5, and for $1 \leq s < t \leq p$, $f_{st}(\mathbf{y}|\boldsymbol{\eta}_{st}, \boldsymbol{\zeta}_{st}) = f_{st}(\mathbf{y}|\boldsymbol{\eta}_{st}, \boldsymbol{\eta}_{ss}, \boldsymbol{\eta}_t)$ satisfies conditions 1-5. Then conditions 1-5 also hold for both $f_1(\mathbf{y}|\boldsymbol{\zeta})$ and $f_2(\mathbf{y}|\boldsymbol{\eta}, \boldsymbol{\zeta})$.*

Recall that $\mathbf{t} = \sqrt{n}(\boldsymbol{\eta} - \hat{\boldsymbol{\eta}}_n)$ and $\mathbf{r} = \sqrt{n}(\boldsymbol{\zeta} - \hat{\boldsymbol{\zeta}}_n)$, then the *Bayesian mosaic* of \mathbf{t} and \mathbf{r} can be written as $\tilde{\pi}_n^*(\mathbf{t}, \mathbf{r}) = \frac{1}{\sqrt{n}} \tilde{\pi}_n(\hat{\boldsymbol{\eta}}_n + \mathbf{t}/\sqrt{n}, \hat{\boldsymbol{\zeta}}_n + \mathbf{r}/\sqrt{n})$. Applying Lemma 3.5 and Theorem 3.3, we know that if the requirements of Lemma 3.5 are satisfied, with $P_{\boldsymbol{\theta}_0}$ -probability one

$$\lim_{n \rightarrow \infty} \int \int \left| \tilde{\pi}_n^*(\mathbf{t}, \mathbf{r}) - \phi\left(\mathbf{t} \mid -(\mathbf{I}_0^{11})^{-1} \mathbf{I}_0^{12} \mathbf{r}, (\mathbf{I}_0^{11})^{-1}\right) \phi\left(\mathbf{r} \mid \boldsymbol{\mu}_n, \tilde{\mathbf{I}}_0^{-1}\right) \right| d\mathbf{r} d\mathbf{t} = 0,$$

where $\tilde{\mathbf{I}}_0 = -\mathbb{E}_{\boldsymbol{\theta}_0} \nabla_{\boldsymbol{\zeta}}^2 \ell_1(\boldsymbol{\zeta}, \mathbf{y})|_{\boldsymbol{\theta}=\boldsymbol{\theta}_0}$, $\mathbf{I}_0^{11} = -\mathbb{E}_{\boldsymbol{\theta}_0} \nabla_{\boldsymbol{\eta}}^2 \ell_2(\boldsymbol{\eta}, \boldsymbol{\zeta}, \mathbf{y})|_{\boldsymbol{\theta}=\boldsymbol{\theta}_0}$ and $\mathbf{I}_0^{12} = -\mathbb{E}_{\boldsymbol{\theta}_0} \nabla_{\boldsymbol{\zeta}} \nabla_{\boldsymbol{\eta}} \ell_2(\boldsymbol{\eta}, \boldsymbol{\zeta}, \mathbf{y})|_{\boldsymbol{\theta}=\boldsymbol{\theta}_0}$.

To gain more insight on what the asymptotic covariance of $\tilde{\pi}_n^*(\mathbf{t}, \mathbf{r})$ is, we will look at \mathbf{I}_0^{11} , \mathbf{I}_0^{12} and $\tilde{\mathbf{I}}_0$ in more detail. For $j = 1, \dots, p$, we define

$$\boldsymbol{\Sigma}_{jj} = \mathbb{E}_{\boldsymbol{\theta}_0} \nabla_{\boldsymbol{\theta}_{jj}}^2 \ell_{jj}(\boldsymbol{\theta}_{jj}, y_j)|_{\boldsymbol{\theta}=\boldsymbol{\theta}_0}.$$

Since $\ell_1(\boldsymbol{\zeta}, \mathbf{y}) = \sum_{j=1}^p \ell_{jj}(y_j|\boldsymbol{\theta}_{jj})$ and $\boldsymbol{\zeta} = (\boldsymbol{\theta}_{11}, \dots, \boldsymbol{\theta}_{pp})^\top$, it is easy to see that

$$\tilde{\mathbf{I}}_0 = \begin{bmatrix} \boldsymbol{\Sigma}_{11} & \mathbf{0} & \cdots & \mathbf{0} \\ \mathbf{0} & \boldsymbol{\Sigma}_{22} & \cdots & \mathbf{0} \\ \vdots & \vdots & \ddots & \vdots \\ \mathbf{0} & \mathbf{0} & \cdots & \boldsymbol{\Sigma}_{pp} \end{bmatrix}.$$

For $1 \leq s < t \leq p$, we define

$$\boldsymbol{\Sigma}_{st} = \mathbb{E}_{\boldsymbol{\theta}_0} \nabla_{\boldsymbol{\theta}_{st}}^2 \ell_{st}(\boldsymbol{\theta}_{st}, \boldsymbol{\theta}_{ss}, \boldsymbol{\theta}_{tt}, y_s, y_t)|_{\boldsymbol{\theta}=\boldsymbol{\theta}_0}.$$

Since $\ell_2(\boldsymbol{\eta}, \boldsymbol{\zeta}, \mathbf{y}) = \sum_{1 \leq s < t \leq p} \ell_{st}(y_s, y_t | \boldsymbol{\theta}_{st}, \boldsymbol{\theta}_{ss}, \boldsymbol{\theta}_{tt})$ and $\boldsymbol{\eta} = [\boldsymbol{\theta}_{12}, \dots, \boldsymbol{\theta}_{(p-1)p}]^\top$, it is easy to see that

$$\mathbf{I}_0^{11} = \begin{bmatrix} \boldsymbol{\Sigma}_{12} & \mathbf{0} & \cdots & \mathbf{0} \\ \mathbf{0} & \boldsymbol{\Sigma}_{13} & \cdots & \mathbf{0} \\ \vdots & \vdots & \ddots & \vdots \\ \mathbf{0} & \mathbf{0} & \cdots & \boldsymbol{\Sigma}_{(p-1)p} \end{bmatrix}.$$

Note that the $\boldsymbol{\Sigma}_{st}$'s are ordered in a row-major manner on the diagonal of $\boldsymbol{\Sigma}_0$. For $1 \leq s < t \leq p$ and $j = 1, \dots, p$, we define

$$\boldsymbol{\Sigma}_{st,j} = \mathbb{E}_{\boldsymbol{\theta}_0} \nabla_{\boldsymbol{\theta}_{jj}} \nabla_{\boldsymbol{\theta}_{st}} \ell_{st}(\boldsymbol{\theta}_{st}, \boldsymbol{\theta}_{ss}, \boldsymbol{\theta}_{tt}, y_s, y_t) | \boldsymbol{\theta} = \boldsymbol{\theta}_0.$$

It can be shown that

$$\mathbf{I}_0^{12} = \begin{bmatrix} \boldsymbol{\Sigma}_{12,1} & \boldsymbol{\Sigma}_{12,2} & \cdots & \boldsymbol{\Sigma}_{12,p} \\ \boldsymbol{\Sigma}_{13,1} & \boldsymbol{\Sigma}_{13,2} & \cdots & \boldsymbol{\Sigma}_{13,p} \\ \vdots & \vdots & \ddots & \vdots \\ \boldsymbol{\Sigma}_{(p-1)p,1} & \boldsymbol{\Sigma}_{(p-1)p,2} & \cdots & \boldsymbol{\Sigma}_{(p-1)p,p} \end{bmatrix},$$

where $\boldsymbol{\Sigma}_{st,j}$'s are ordered in a row-major manner within their column for $j = 1, \dots, p$. Note that \mathbf{I}_0^{12} is sparse since $\boldsymbol{\Sigma}_{st,j} = \mathbf{0}$ if $j \neq s$ and $j \neq t$.

$\tilde{\mathbf{I}}_0^{-1}$ is the marginal variance for \mathbf{r} . It is block diagonal due to the posterior independence of the *knots*. It can be seen that each block is the Fisher information induced by a univariate marginal data distribution. $(\mathbf{I}_0^{11})^{-1}$ is the conditional variance for \mathbf{t} . It is also block diagonal due to the conditional independence of the *tiles* given the *knots*. Each block is the Fisher information induced by a bivariate marginal data distribution. \mathbf{I}_0^{12} characterizes the connection between *knots* and *tiles*. Its sparsity is due to the fact that $\boldsymbol{\theta}_{st}$ given $\boldsymbol{\theta}_{ss}$ and $\boldsymbol{\theta}_{tt}$ is conditionally independent of other *knots*.

3.3 Asymptotic Properties of the Posterior Mean

Under the same setup of Lemma 3.2, define $\boldsymbol{\zeta}_n^*$ as the posterior mean w.r.t. $\kappa_n(\boldsymbol{\zeta})$, i.e., $\boldsymbol{\zeta}_n^* = \int \boldsymbol{\zeta} \kappa_n(\boldsymbol{\zeta}) d\boldsymbol{\zeta}$. We can prove the following lemma.

Lemma 3.6. *Suppose the conditions for Lemma 3.2 hold and that the prior $\pi(\boldsymbol{\zeta})$ has a finite expectation, then $\lim_{n \rightarrow \infty} \sqrt{n}(\boldsymbol{\zeta}_n^* - \tilde{\boldsymbol{\zeta}}_n) = 0$ with $P_{\boldsymbol{\theta}_0}$ -probability one.*

Lemma 3.6 is a multivariate version of Theorem 4.3 in Ghosh et al. [2007]. It states that the posterior mean is approximately the same as the MLE when n is large.

Now we will investigate sampling from *tile conditionals* by directly plugging in the posterior mean of the *knots*. Under the same setup of Theorem 3.3, if we plug ζ_n^* into the conditional density $\tau_n(\boldsymbol{\eta}|\zeta)$, we will get the following posterior distribution

$$\tau_n(\boldsymbol{\eta}|\zeta_n^*)\kappa_n(\zeta),$$

which is different from the exact *Bayesian mosaic* posterior. Recalling that $\mathbf{t} = \sqrt{n}(\boldsymbol{\eta} - \hat{\boldsymbol{\eta}}_n)$ and letting $\pi_{n,3}^*(\mathbf{t}) = \frac{1}{\sqrt{n}}\tau_n(\hat{\boldsymbol{\eta}}_n + \mathbf{t}/\sqrt{n}|\zeta_n^*)$, the following theorem states that $\pi_{n,3}^*(\mathbf{t})$ is also asymptotic normal in a slightly weaker sense.

Theorem 3.7. *Suppose that the conditions for Theorem 3.3 hold that the prior $\pi(\zeta)$ has a finite expectation, then*

$$\int \left| \pi_{n,3}^*(\mathbf{t}) - \phi\left(\mathbf{t} \middle| -(\mathbf{I}_0^{11})^{-1} \mathbf{I}_0^{12} \boldsymbol{\mu}_n, (\mathbf{I}_0^{11})^{-1}\right) \right| d\mathbf{t} \xrightarrow{P_{\theta_0}} 0. \quad (10)$$

Note that the integral in (10) converges to zero in probability, which is slightly weaker than the almost surely convergence in Theorem 3.3. Moreover, Theorem 3.3 implies that

$$\lim_{n \rightarrow \infty} \int \left| \int \pi_n^*(\mathbf{t}, \mathbf{r}) d\mathbf{r} - \phi\left(\mathbf{t} \middle| -(\mathbf{I}_0^{11})^{-1} \mathbf{I}_0^{12} \boldsymbol{\mu}_n, (\mathbf{I}_0^{11})^{-1} + \boldsymbol{\Lambda}_0\right) \right| d\mathbf{t} = 0,$$

where

$$\boldsymbol{\Lambda}_0 = \mathbf{I}_0^{12} (\mathbf{I}_0^{11})^{-1} \tilde{\mathbf{I}}_0 (\mathbf{I}_0^{11})^{-1} \mathbf{I}_0^{21}$$

is positive semi-definite. This indicates that plugging in the posterior mean leads to some under-estimation of uncertainty as expected.

3.4 Asymptotic Bound on Computational Complexity

We finish this section by investigating the per-iteration computational complexity of sampling from *Bayesian mosaic* when the data are discrete. We start by analyzing sampling from the *knot marginals*. Recall

$$\kappa_j(\boldsymbol{\theta}_{jj}) \propto e^{\sum_{i=1}^n \ell_{jj}(\boldsymbol{\theta}_{jj}, y_{ij})} \pi_{jj}(\boldsymbol{\theta}_{jj}). \quad (11)$$

For discrete data, we assume the cardinality of $\{y_{1j}, \dots, y_{nj}\}$ is $K \in \mathbb{N}_1$ and that $y_{i_1j}, \dots, y_{i_Kj}$ are K unique values of y_{1j}, \dots, y_{nj} . For $k = 1, \dots, K$, we define $n_k = \sum_{i=1}^n \mathbb{1}\{y_{ij} = y_{i_kj}\}$. Then (11) can be written as

$$\kappa_j(\boldsymbol{\theta}_{jj}) \propto e^{\sum_{k=1}^K n_k \ell_{jj}(\boldsymbol{\theta}_{jj}, y_{i_kj})} \pi_{jj}(\boldsymbol{\theta}_{jj}).$$

Clearly the per-iteration computational complexity of sampling from $\kappa_{n,j}(\boldsymbol{\theta}_{jj})$ is dominated by evaluating $\sum_{k=1}^K n_k \ell_{jj}(\boldsymbol{\theta}_{jj}, y_{i_kj})$, which scales linearly with K . It is easily seen that K is bounded by $\max_{1 \leq i \leq n} y_{ij} - \min_{1 \leq i \leq n} y_{ij}$. For simplicity, we assume that the data only take positive values, which implies that K is upper-bounded by $\max_{1 \leq i \leq n} y_{ij}$, whose asymptotic distribution is studied in extreme value theory. Since this asymptotic distribution is model specific, we use the rounded multivariate Gaussian model of Canale and Dunson [2011] as an illustration. This model is a special case of the multivariate latent Gaussian model defined in (1) with $h_j(y_j|x_j) = \mathbb{1}\{x_j > 0\} \lceil x_j \rceil$. Basically $h_j(y_j|x_j)$ is a rounding function that rounds x_j to the smallest integer larger than it while mapping all x_j below 0 to 0.

Lemma 3.8. *Consider model (1) with $h_j(y_j|x_j) = \mathbb{1}\{x_j > 0\} \lceil x_j \rceil$, for $j = 1, \dots, p$, we have that $\forall \delta > 0, \exists N \in \mathbb{N}_1$ such that $\forall n > N$,*

$$\text{pr} \left[\max_{1 \leq i \leq n} y_{ij} < \sqrt{\sigma_{jj}} \left(\frac{2\delta}{\sqrt{\log n}} + \sqrt{2 \log n} \right) + \mu_j + 1 \right] > e^{-\exp(-\delta/2)}. \quad (12)$$

Intuitively, (12) implies that K is at most $O(\sqrt{\log n})$ with high probability. Similarly, one can show that the computational complexity of evaluating the data likelihood of any bivariate marginal distribution is at most $O(\log n)$.

To summarize, we have shown that the per-iteration computational complexity is linear in the cardinality of the discrete observations. This cardinality can be bounded by the data maxima; hence its asymptotic distribution can be analyzed using standard extreme value theory. We have shown that the per-iteration complexity is at most $O(\log n)$ with high probability for the rounded multivariate Gaussian model.

4 Experiments

The performance of *Bayesian Mosaic* will be illustrated via two simulation studies and a citation network application. The first simulation study demonstrates the superiority of *Bayesian Mosaic* over DA-MCMC for imbalanced

count data. The second simulation study demonstrates that *Bayesian Mosaic* achieves similar accuracy with a provably more scalable computational complexity for large balanced count data. *Bayesian mosaic* is also applied to a citation count dataset to infer the overlapping structure of a group of researchers’ interests.

All experiments are conducted in R on a machine with 12 3.50 GHz Intel(R) Xeon(R) CPU E5-1650 v3 processors. All results are based on 100 replicate experiments.

4.1 Multivariate log-Gaussian Mixture of Poisson

In the first simulation study, we considered a special case of multivariate latent Gaussian models with $h_j(y_j|x_j)$ being the density function of a Poisson distribution whose rate parameter equals e^{x_j} . We generated 100 datasets for each unique data dimensionality p in $\{3, 5, 7\}$. We fixed the sample size to be 10000. For each synthetic dataset we randomly generated $\boldsymbol{\mu}$ and $\boldsymbol{\Sigma}$ from some distribution so that the simulated dataset has an excessive amount of zeros. More specifically, for $j = 1, \dots, p$, we generated μ_j from $\text{Unif}(-4, -3)$ and σ_{jj} from $\text{Unif}(0.5, 1)$. We randomly generated a correlation matrix from the standard LKJ distribution Lewandowski et al. [2009] and then combined this correlation matrix with $\sigma_{11}, \dots, \sigma_{pp}$ into $\boldsymbol{\Sigma}$. Roughly 90% of the simulated data entries are zeros.

We used weakly-informative priors in both simulation studies. Specifically, for $j = 1, \dots, p$,

$$\pi_{jj}(\mu_j, \sigma_{jj}) \propto \sigma_{jj}^{-1/2} \mathbb{1}\{|\mu_j| < A, 0 < \sigma_{jj} < B\},$$

where $A > 0$ and $B > 0$. For $1 \leq s < t \leq p$,

$$\pi_{jj}(\sigma_{st}|\mu_s, \sigma_{ss}, \mu_t, \sigma_{tt}) \propto \mathbb{1}\{|\sigma_{st}| < \sqrt{\sigma_{ss}\sigma_{tt}}\}.$$

The propriety of the posterior is guaranteed since the support of the prior is compact. Moreover, for sufficiently large A and B , the posterior becomes insensitive to the choice of A and B [Gelman et al., 2006]. We let $A = 100$ and $B = 10$. We used a similar prior specification in citation count application.

Normal independent MH sampler was implemented for sampling the *knot marginals* for 200 iterations with the first 100 as burn-in. We then approximated *tile conditionals* via Laplace approximation and drew 100 samples of the *tiles* from the resulting conditional Gaussian distribution given

Table 1: Mean Square Error Comparison.¹

		$p = 3$	$p = 5$	$p = 7$
<i>Bayesian Mosaic</i>	ρ	6.79 (9.76)	5.78 (8.14)	5.62 (7.92)
	s	5.9 (9.54)	5.86 (9.13)	5.86 (8.63)
	μ	1.74 (2.39)	1.74 (2.71)	1.7 (2.52)
DA-MCMC	ρ	8.41 (15.3)	9.93 (14.8)	10 (14.4)
	s	150 (1892)	303 (3020)	443 (3744)
	μ	54.9 (345)	123 (522)	126 (571)

Table 2: Empirical Coverage Comparison

		$p = 3$	$p = 5$	$p = 7$
<i>Bayesian Mosaic</i>	ρ	95%	93.9%	93%
	s	93.7%	93.4%	94.1%
	μ	93%	92.6%	93.7%
DA-MCMC	ρ	64%	56.8%	59.3%
	s	41.7%	32.4%	31.1%
	μ	37%	24.8%	24.9%

the previous draws of the *knots*. On average, a single run with the computation distributed to 11 parallel workers took 90 seconds for $p = 3$, 126 seconds for $p = 5$ and 227 seconds for $p = 7$. As a comparison, we ran DA-MCMC sampler for the 5 times the amount of time with the computation tasks within each iteration distributed to 11 parallel workers as well. In both simulation studies, we gave DA-MCMC an unfair advantage by initializing the parameter values at the true values.

We first compared accuracies of estimating the model parameters w.r.t. square error loss. Average MSE within each group are presented in Table 1, where the number in the parenthesis is the standard error. It can be clearly seen that the estimates based on *Bayesian mosaic* outperforms those based on DA-MCMC samples in terms of square error loss.

We evaluated *Bayesian mosaic*'s performance in quantifying the uncertainty through the empirical coverage (EC) of credible intervals. Average EC's are presented in Table 2. The empirical coverages of *Bayesian mosaic* are close to 95%, indicating good uncertainty quantification, whereas the

¹All numbers have been multiplied by 100.

Table 3: Performance Comparison

		MSE ²	EC
<i>Bayesian Mosaic</i>	ρ	1.07 (1.59)	90.2%
	s	3.23 (4.33)	94%
	μ	1.45 (1.89)	91.5%
DA-MCMC	ρ	0.91 (1.37)	94.2%
	s	3.29 (4.34)	95.3%
	μ	1.45 (1.91)	91.3%

empirical coverages based on DA-MCMC are terribly off.

4.2 Rounded Multivariate Gaussian

In the second simulation study, we considered the rounded multivariate Gaussian model [Canale and Dunson, 2011] given in §3.4. We fixed the sample size to be 10000, data dimensionality $p = 4$ and generated 100 datasets. For each synthetic dataset we randomly generated $\boldsymbol{\mu}$ and $\boldsymbol{\Sigma}$ from some distribution so that the simulated data are well balanced (majority of the data entries are non-zero). More specifically, for $j = 1, \dots, p$, we generated μ_j from $\text{Unif}(4, 5)$ and σ_{jj} from $\text{Unif}(1, 1.5)$. The analysis was done exactly as in §4.1.

The average MSE and EC are summarized in Table 3. DA-MCMC seems to do slightly better than *Bayesian mosaic*. But the difference in performance is marginal. Due to the limitation of computation power for DA-MCMC, we did not do experiments with larger sample size n . According to our discussion in §3.4, the per-iteration computational complexity of *Bayesian mosaic* is roughly $O(\log n)$ while that of DA-MCMC is $O(n)$. This implies that *Bayesian mosaic* should be favored in large sample size applications even if data are well balanced.

4.3 Citation Network Application

In this study, we considered a real-world citation network dataset [Tang et al., 2008] that contains papers and citation relationships from a computer science bibliography website called DBLP. Our goal is to study the overlapping structure of a group of researchers' interests. Intuitively, two researchers who

²All numbers have been multiplied by 10^4 .

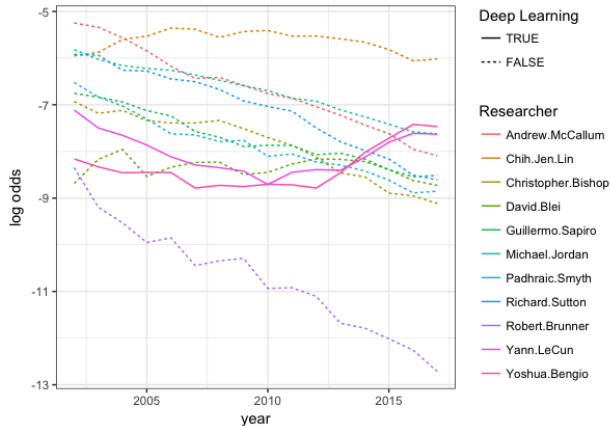


Figure 2: Visualizing the posterior mean of μ_t 's by researchers.

have many research interests in common tend to be cited together more frequently. Meanwhile, we also want to see how is the research impact of these researchers varying in time. We hand-picked 11 active researchers³ in the machine learning community.

In processing the database, we focused on the machine learning literature and removed irrelevant papers. When counting the number of citations, we ignored papers co-authored by multiple researchers in our hand-picked group. The final dataset contains roughly 80000 11-dimensional observations with each one being the number of citations of a certain paper go to each of the 11 researchers. We used i as the index for papers and j as the index for the researchers. Letting t_i be the year paper i was published and n_{jt} be the total number of publications of researcher j up to year t , we used the following model

$$y_{ij} \stackrel{iid}{\sim} \text{Binomial}(n_{jt_i}, \text{logit}^{-1}(x_{ij})) \text{ for } j = 1, \dots, p,$$

$$\mathbf{x}_i \stackrel{iid}{\sim} N(\boldsymbol{\mu}_{t_i}, \boldsymbol{\Sigma}), \quad \boldsymbol{\mu}_t \stackrel{iid}{\sim} N(\boldsymbol{\mu}_0, \mathbf{D}),$$

where $\mathbf{x}_i = (x_{i1}, \dots, x_{ip})^\top$, $p = 11$ and \mathbf{D} is a diagonal matrix with the diagonal elements being positive. The model parameters are $\boldsymbol{\mu}_0$, $\boldsymbol{\Sigma}$ and \mathbf{D} whereas $\boldsymbol{\mu}_t$'s are random effects.

³Michael Jordan, Robert Brunner, Yann LeCun, Andrew McCallum, Chih-Jen Lin, Christopher Bishop, Yoshua Bengio, David Blei, Padhraic Smyth, Richard Sutton, Guillermo Sapiro

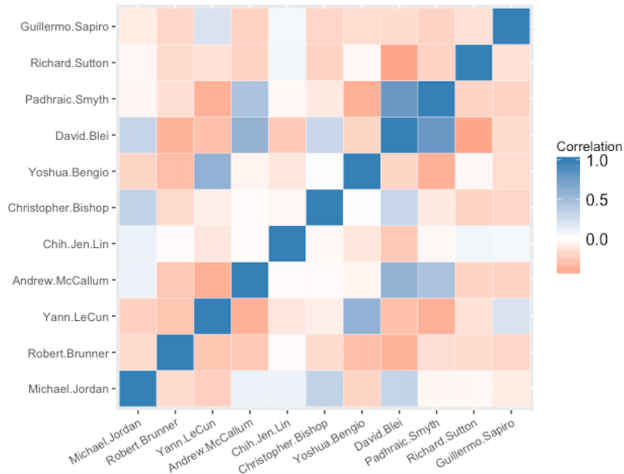


Figure 3: Visualizing the correlation matrix induced by Σ .

After integrating out μ_t 's and x_i 's, y_i 's are no longer independent. It is easy to check that the above model is *mosaic-type* in the generalized *Bayesian mosaic* framework of §2.6. Normal random walk MH sampler was implemented for sampling the *knot marginals* for 40000 iterations with the first 20000 as burn-in and thinning the rest into 500 samples. In sampling the *tiles*, we used the plug-in approach discussed in §2.4 and sampled from the resulted *tile conditionals* via MH. For each *tile*, we ran the MH sampler 10000 iterations with the first 5000 as burn-in and thinned the rest into 500 final samples. The entire sampling process took around 5 hours with the jobs distributed to 11 parallel workers.

Figure 2 visualizes the posterior mean of the random effects μ_t 's by different researchers. Intuitively, μ_t is a vector of the average log-odds of a single paper citing these researchers. Interestingly, while most of the researchers' log-odds of being cited is decreasing, the only two exceptions are both working on deep learning.

We also computed the posterior mean of Σ (after correction). The induced correlation matrix is visualized via a heatmap in Figure 3. Clearly, some researchers are more likely to be cited together compared to the others, indicating their strong overlapping research interests. For instance, Yann LeCun and Yoshua Bengio have a stronger correlation since they are both studying deep learning. There are researchers whose research interests seem to overlap with many others, e.g., David Blei. Also, there are researchers whose

research interests seem to be unique in this selected group, e.g., Richard Sutton.

A Proofs

Whenever we write $\lim_{n \rightarrow \infty} a_n = a_0$, we mean the limit holds with P_{θ_0} -probability one. We will omit the phrase “with P_{θ_0} -probability one” for succinctness.

A.1 Proof of Lemma 3.1

Since P_ψ is *mosaic-type*, from Definition 2.1, we have ψ_{st} , $1 \leq t \leq s \leq p$ such that

$$\psi = [\psi_{12}^\top, \dots, \psi_{(p-1)p}^\top, \psi_{11}^\top, \dots, \psi_{pp}^\top]^\top.$$

For $j = 1, \dots, p$, the density of the univariate marginal distribution of P_ψ is $f_{0,jj}(x_j | \psi_{jj})$. And for $1 \leq t < s \leq p$, the density of the bivariate marginal data distribution of P_ψ is $f_{0,st}(x_s, x_t | \psi_{st}, \psi_{ss}, \psi_{tt})$. Introduce

$$\theta = [\psi_{12}^\top, \dots, \psi_{(p-1)p}^\top, \psi_{11}^\top, \mu_1^\top, \dots, \psi_{pp}^\top, \mu_p^\top]^\top,$$

and let $\theta_{st} = \psi_{st}$ for $1 \leq s < t \leq p$ and $\theta_{jj} = (\psi_{jj}^\top, \mu_j^\top)^\top$ for $j = 1, \dots, p$. From (3.1), it can be shown that

$$\begin{aligned} & \int \cdots \int f(\mathbf{y} | \boldsymbol{\mu}, \boldsymbol{\psi}) dy_2 \cdots dy_p \\ &= \int f_0(\mathbf{x} | \boldsymbol{\psi}) g_1(y_1 | x_1, \boldsymbol{\mu}_1) \prod_{j=2}^p \left[\int g_j(y_j | x_j, \boldsymbol{\mu}_j) dy_j \right] d\mathbf{x} \\ &= \int f_{0,11}(x_1 | \psi_{11}) g_1(y_1 | x_1, \boldsymbol{\mu}_1) dx_1 \\ &= f_{11}(y_1 | \boldsymbol{\theta}_{11}). \end{aligned}$$

Similarly, one can show that there exists a collection of density functions $\{f_{jj}(y_j | \boldsymbol{\theta}_{jj})\}$ such that for $j = 2, \dots, p$, the density of the univariate marginal distribution of $P_{\boldsymbol{\mu}, \boldsymbol{\psi}}$ is $f_{jj}(y_j | \boldsymbol{\theta}_{jj})$. And that there exists a collection of density functions $\{f_{st}(y_s, y_t | \boldsymbol{\theta}_{st}, \boldsymbol{\theta}_{ss}, \boldsymbol{\theta}_{tt})\}$ such that for $1 \leq t < s \leq p$, the density of the bivariate marginal data distribution of $P_{\boldsymbol{\mu}, \boldsymbol{\psi}}$ is $f_{st}(y_s, y_t | \boldsymbol{\theta}_{st}, \boldsymbol{\theta}_{ss}, \boldsymbol{\theta}_{tt})$. Hence $P_{\boldsymbol{\mu}, \boldsymbol{\psi}}$ is also *Mosaic-type*.

A.2 Taylor Expansions & Upper Bounds

We will find the limit and derive an upper bound for the Taylor expansion of $L_n(\boldsymbol{\eta}, \boldsymbol{\zeta})$, which will be used in later proofs.

Lemma A.1. *Letting $\boldsymbol{\alpha}$ be a d -dimensional multi-index for \mathbf{x} , consider $M_{\boldsymbol{\alpha}} < \infty$ for all $\boldsymbol{\alpha}$ such that $|\boldsymbol{\alpha}| = 3$. Then for any positive definite matrix $\boldsymbol{\Lambda}$, we can find $\delta > 0$ such that when $|\mathbf{x}| < \sqrt{n}\delta$,*

$$\left| \sum_{|\boldsymbol{\alpha}|=3} M_{\boldsymbol{\alpha}} \frac{\mathbf{x}^{\boldsymbol{\alpha}}}{\sqrt{n}} \right| < \frac{1}{2} \mathbf{x}^{\top} \boldsymbol{\Lambda} \mathbf{x}.$$

Proof. It is easily seen that

$$\left| \sum_{|\boldsymbol{\alpha}|=3} M_{\boldsymbol{\alpha}} \frac{\mathbf{x}^{\boldsymbol{\alpha}}}{\sqrt{n}} \right| < \sum_{|\boldsymbol{\alpha}|=3} M_{\boldsymbol{\alpha}} \left| \frac{\mathbf{x}^{\boldsymbol{\alpha}}}{\sqrt{n}} \right|.$$

Consider $\boldsymbol{\alpha} = (\alpha_1, \dots, \alpha_d)$ where $|\boldsymbol{\alpha}| = 3$, and suppose α_{j_1} is the first non-zero index. Since $|\mathbf{x}| < \sqrt{n}\delta$, we have $\frac{|x_{j_1}|}{\sqrt{n}} < \delta$. Assume that α_{j_2} and α_{j_3} are the other two non-zero indices, note that we allow $j_2 = j_3$. We have

$$\left| \frac{\mathbf{x}^{\boldsymbol{\alpha}}}{\sqrt{n}} \right| < \delta |x_{j_2} x_{j_3}| \leq \frac{\delta}{2} (x_{j_2}^2 + x_{j_3}^2).$$

Doing this for all $\boldsymbol{\alpha}$ such that $|\boldsymbol{\alpha}| = 3$, it can be shown that

$$\sum_{|\boldsymbol{\alpha}|=3} M_{\boldsymbol{\alpha}} \left| \frac{\mathbf{x}^{\boldsymbol{\alpha}}}{\sqrt{n}} \right| < \frac{\delta}{2} \mathbf{x}^{\top} \boldsymbol{\Psi} \mathbf{x},$$

where $\boldsymbol{\Psi}$ is some diagonal matrix with all diagonal elements being positive. Since $\boldsymbol{\Lambda}$ is positive definite, we can always find $\delta > 0$ so that $\boldsymbol{\Lambda} - \delta\boldsymbol{\Psi}$ is also positive definite, which implies that for any $\mathbf{x} \in \mathbb{R}^d$,

$$\frac{1}{2} \mathbf{x}^{\top} \boldsymbol{\Lambda} \mathbf{x} - \frac{\delta}{2} \mathbf{x}^{\top} \boldsymbol{\Psi} \mathbf{x} = \frac{1}{2} \mathbf{x}^{\top} (\boldsymbol{\Lambda} - \delta\boldsymbol{\Psi}) \mathbf{x} > 0.$$

□

Recall that $\mathbf{t} = \sqrt{n}(\boldsymbol{\eta} - \hat{\boldsymbol{\eta}}_n)$ and $\mathbf{r} = \sqrt{n}(\boldsymbol{\zeta} - \hat{\boldsymbol{\zeta}}_n)$. Letting $\boldsymbol{\alpha}$ be a $d_{\boldsymbol{\eta}}$ -dimensional *multi-index* for \mathbf{t} and $\boldsymbol{\beta}$ be a $d_{\boldsymbol{\zeta}}$ -dimensional *multi-index* for

\mathbf{r} , we expand the Taylor series for $L_n(\hat{\boldsymbol{\eta}}_n + \mathbf{t}/\sqrt{n}, \hat{\boldsymbol{\zeta}}_n + \mathbf{r}/\sqrt{n}) - L_n(\hat{\boldsymbol{\eta}}_n, \hat{\boldsymbol{\zeta}}_n)$ and get

$$\begin{aligned} & L_n(\hat{\boldsymbol{\eta}}_n + \mathbf{t}/\sqrt{n}, \hat{\boldsymbol{\zeta}}_n + \mathbf{r}/\sqrt{n}) - L_n(\hat{\boldsymbol{\eta}}_n, \hat{\boldsymbol{\zeta}}_n) \\ &= \frac{1}{2} \begin{bmatrix} \mathbf{t} \\ \mathbf{r} \end{bmatrix}^\top \frac{1}{n} L_n^{(2)}(\hat{\boldsymbol{\eta}}_n, \hat{\boldsymbol{\zeta}}_n) \begin{bmatrix} \mathbf{t} \\ \mathbf{r} \end{bmatrix} + R_n(\mathbf{t}, \mathbf{r}), \end{aligned} \quad (13)$$

where $\boldsymbol{\eta}'_n$ is between $\hat{\boldsymbol{\eta}}_n + \mathbf{t}/\sqrt{n}$ and $\hat{\boldsymbol{\eta}}_n$, $\boldsymbol{\zeta}'_n$ is between $\hat{\boldsymbol{\zeta}}_n + \mathbf{r}/\sqrt{n}$ and $\hat{\boldsymbol{\zeta}}_n$ and

$$R_n(\mathbf{t}, \mathbf{r}) = \sum_{|\boldsymbol{\alpha}|+|\boldsymbol{\beta}|=3} \frac{1}{n\boldsymbol{\alpha}!} \partial^\alpha \partial^\beta L_n(\boldsymbol{\eta}'_n, \boldsymbol{\zeta}'_n) \frac{\mathbf{t}^\alpha \mathbf{r}^\beta}{\sqrt{n}}.$$

Letting $\hat{\mathbf{I}}_n = -\frac{1}{n} L_n^{(2)}(\hat{\boldsymbol{\eta}}_n, \hat{\boldsymbol{\lambda}}_n)$ and $\hat{\mathbf{I}}_n = \begin{bmatrix} \hat{\mathbf{I}}_n^{11} & \hat{\mathbf{I}}_n^{12} \\ \hat{\mathbf{I}}_n^{21} & \hat{\mathbf{I}}_n^{22} \end{bmatrix}$, (13) can be written as

$$\begin{aligned} & L_n(\hat{\boldsymbol{\eta}}_n + \mathbf{t}/\sqrt{n}, \hat{\boldsymbol{\zeta}}_n + \mathbf{r}/\sqrt{n}) - L_n(\hat{\boldsymbol{\eta}}_n, \hat{\boldsymbol{\zeta}}_n) \\ &= -\frac{1}{2} \mathbf{t}^\top \hat{\mathbf{I}}_n^{11} \mathbf{t} - \frac{1}{2} \mathbf{r}^\top \hat{\mathbf{I}}_n^{22} \mathbf{r} - \mathbf{t}^\top \hat{\mathbf{I}}_n^{12} \mathbf{r} + R_n(\mathbf{t}, \mathbf{r}). \end{aligned} \quad (14)$$

Corollary A.2. *If conditions 1-5 hold for $f_2(\mathbf{y}|\boldsymbol{\eta}, \boldsymbol{\zeta})$, then $\exists \delta > 0$ such that for all \mathbf{t} and \mathbf{r} satisfying $\left\| \begin{bmatrix} \mathbf{t}/\sqrt{n} \\ \mathbf{r}/\sqrt{n} \end{bmatrix} \right\| < \delta$, the followings are true:*

- i) For any fixed \mathbf{t} and \mathbf{r} , $\lim_{n \rightarrow \infty} R_n(\mathbf{t}, \mathbf{r}) = 0$.*
- ii) For any positive definite matrix $\boldsymbol{\Lambda}$, $\exists N \in \mathbb{N}_1$ such that $\forall n > N$,*

$$|R_n(\mathbf{t}, \mathbf{r})| < \begin{bmatrix} \mathbf{t} \\ \mathbf{r} \end{bmatrix}^\top \boldsymbol{\Lambda} \begin{bmatrix} \mathbf{t} \\ \mathbf{r} \end{bmatrix}. \quad (15)$$

Proof. From condition 2, for some $\delta' > 0$ we have

$$\sup_{\mathbf{z} \in \mathcal{B}(\mathbf{z}_0, \delta')} |\partial^\alpha \ell_2(\boldsymbol{\eta}, \boldsymbol{\zeta}, \mathbf{y})| \leq M_{\alpha,2}(\mathbf{y}),$$

and $\mathbb{E}_{\boldsymbol{\theta}_0} M_{\alpha,2}(\mathbf{y}) < \infty$. Letting $\delta < \delta'$, we have

$$\left| \sum_{|\boldsymbol{\alpha}|+|\boldsymbol{\beta}|=3} \frac{1}{n\boldsymbol{\alpha}!} \partial^\alpha \partial^\beta L_n(\boldsymbol{\eta}'_n, \boldsymbol{\zeta}'_n) \frac{\mathbf{t}^\alpha \mathbf{r}^\beta}{\sqrt{n}} \right| < \sum_{|\boldsymbol{\alpha}|+|\boldsymbol{\beta}|=3} \frac{1}{n\boldsymbol{\alpha}!} \sum_{i=1}^n M_{\alpha,2}(\mathbf{y}_i) \frac{\mathbf{t}^\alpha \mathbf{r}^\beta}{\sqrt{n}}.$$

From strong law of large numbers (SLLN) we know that $\lim_{n \rightarrow \infty} \frac{1}{n} \sum_{i=1}^n M_{\alpha,2}(\mathbf{y}_i) = \mathbb{E}_{\theta_0} M_{\alpha,2}(\mathbf{y})$, hence $\exists N_1 \in \mathbb{N}_1$ such that $\forall n > N_1$,

$$\left| \sum_{|\alpha|+|\beta|=3} \frac{1}{n\alpha!} \partial^\alpha \partial^\beta L_n(\boldsymbol{\eta}'_n, \boldsymbol{\zeta}'_n) \frac{\mathbf{t}^\alpha \mathbf{r}^\beta}{\sqrt{n}} \right| < 2 \sum_{|\alpha|+|\beta|=3} \frac{1}{\alpha!} \mathbb{E}_{\theta_0} M_{\alpha,2}(\mathbf{y}) \frac{\mathbf{t}^\alpha \mathbf{r}^\beta}{\sqrt{n}}.$$

Apparently, for fixed \mathbf{t} and \mathbf{r} ,

$$\lim_{n \rightarrow \infty} |R_n(\mathbf{t}, \mathbf{r})| < \lim_{n \rightarrow \infty} 2 \sum_{|\alpha|+|\beta|=3} \frac{1}{\alpha!} \mathbb{E}_{\theta_0} M_{\alpha,2}(\mathbf{y}) \frac{\mathbf{t}^\alpha \mathbf{r}^\beta}{\sqrt{n}} = 0.$$

Therefore $\lim_{n \rightarrow \infty} |R_n(\mathbf{t}, \mathbf{r})| = 0$.

Applying Lemma A.1, we could find $\delta < \delta'$ and $N_2 \in \mathbb{N}_1$ such that $\forall n > \max\{N_1, N_2\}$,

$$\left| 2 \sum_{|\alpha|+|\beta|=3} \frac{1}{\alpha!} \mathbb{E}_{\theta_0} M_{\alpha,2}(\mathbf{y}) \frac{\mathbf{t}^\alpha \mathbf{r}^\beta}{\sqrt{n}} \right| < \begin{bmatrix} \mathbf{t} \\ \mathbf{r} \end{bmatrix}^\top \boldsymbol{\Lambda} \begin{bmatrix} \mathbf{t} \\ \mathbf{r} \end{bmatrix}.$$

Letting $N = \max\{N_1, N_2\}$ finishes the proof. \square

A.3 Proof of Lemma A.3

For $\delta > 0$, we define $A_{n,1}(\delta) = \{\mathbf{r} : \|\mathbf{r}\| < \sqrt{n}\delta\}$, $A_{n,2}(\delta) = \{\mathbf{r} : \|\mathbf{r}\| > \sqrt{n}\delta\}$, $B_{n,1}(\delta) = \{\mathbf{t} : \|\mathbf{t}\| < \sqrt{n}\delta\}$ and $B_{n,2}(\delta) = \{\mathbf{t} : \|\mathbf{t}\| > \sqrt{n}\delta\}$. We first provide a lemma that will be used in our later proof of the main result.

Lemma A.3. *Suppose that conditions 1-5 hold for $f_2(\mathbf{y}|\boldsymbol{\eta}, \boldsymbol{\zeta})$ and the prior density $\pi(\boldsymbol{\eta}|\boldsymbol{\zeta})$ is continuous and positive at $[\boldsymbol{\eta}_0^0]$, then $\exists \delta_t > 0$, $\delta_r > 0$ and $N \in \mathbb{N}_1$ such that the followings are true:*

- For any fixed \mathbf{t} and \mathbf{r} , with P_{θ_0} -probability one

$$\begin{aligned} & \lim_{n \rightarrow \infty} \pi_{n,2}^*(\mathbf{t}|\mathbf{r}) \mathbb{1}\{\mathbf{r} \in A_{n,1}(\delta_r), \mathbf{t} \in B_{n,1}(\delta_t)\} \\ & = \phi\left(\mathbf{t} \middle| -(\mathbf{I}_0^{11})^{-1} \mathbf{I}_0^{12} \mathbf{r}, (\mathbf{I}_0^{11})^{-1}\right). \end{aligned} \quad (16)$$

- $\exists \epsilon > 0$ and $c(\delta_r, \delta_t) > 0$ such that

$$\pi_{n,2}^*(\mathbf{t}|\mathbf{r}) \mathbb{1}\{\mathbf{r} \in A_{n,1}(\delta_r), \mathbf{t} \in B_{n,2}(\delta_t)\} < \frac{|4\pi \mathbf{I}_0^{11}|^{-1/2}}{c(\delta_r, \delta_t)} \exp\{-n\epsilon\}. \quad (17)$$

Proof. The proof consists of the following four steps.

Step 1 In this step we will find the limit of the normalizing constant. The constant is

$$a_n(\mathbf{r}) = \int g_n(\mathbf{t}, \mathbf{r}) d\mathbf{t}, \quad (18)$$

where

$$g_n(\mathbf{t}, \mathbf{r}) = \exp \left\{ L_n(\hat{\boldsymbol{\eta}}_n + \mathbf{t}/\sqrt{n}, \hat{\boldsymbol{\zeta}}_n + \mathbf{r}/\sqrt{n}) - L_n(\hat{\boldsymbol{\eta}}_n, \hat{\boldsymbol{\zeta}}_n) \right\} \\ \times \pi(\hat{\boldsymbol{\eta}}_n + \mathbf{t}/\sqrt{n} | \hat{\boldsymbol{\zeta}}_n + \mathbf{r}/\sqrt{n}) \mathbb{1}\{\mathbf{r} \in A_{n,1}(\delta_r)\}.$$

We can find the limit of $a_n(\mathbf{r})$ by finding the limits of $\int g_n(\mathbf{t}, \mathbf{r}) \mathbb{1}\{\mathbf{t} \in B_{n,1}(\delta_t)\} d\mathbf{t}$ and of $\int g_n(\mathbf{t}, \mathbf{r}) \mathbb{1}\{\mathbf{t} \in B_{n,2}(\delta_t)\} d\mathbf{t}$, since $a_n(\mathbf{r})$ is the sum of the these two integrals. We start with the first one.

The Taylor expansion of $L_n(\hat{\boldsymbol{\eta}}_n + \mathbf{t}/\sqrt{n}, \hat{\boldsymbol{\zeta}}_n + \mathbf{r}/\sqrt{n}) - L_n(\hat{\boldsymbol{\eta}}_n, \hat{\boldsymbol{\zeta}}_n)$ is given in (14). Applying Corollary A.2, and since $\|[\frac{\mathbf{t}}{\mathbf{r}}]\| \leq \|\mathbf{r}\| + \|\mathbf{t}\|$, we could find $\delta_t > 0$ and $N_{11} \in \mathbb{N}_1$ such that $\forall \mathbf{t} \in B_{n,1}(\delta_t)$, $\forall \mathbf{r} \in A_{n,1}(\delta_r)$ and $\forall n > N_{11}$,

$$|R_n(\mathbf{t}, \mathbf{r})| < \frac{1}{8} [\frac{\mathbf{t}}{\mathbf{r}}]^\top \mathbf{I}_0 [\frac{\mathbf{t}}{\mathbf{r}}]. \quad (19)$$

From condition 5, we know that $\lim_{n \rightarrow \infty} \hat{\boldsymbol{\eta}}_n = \boldsymbol{\eta}_0$ and $\lim_{n \rightarrow \infty} \hat{\boldsymbol{\zeta}}_n = \boldsymbol{\zeta}_0$. Applying condition 3, we can show that $\lim_{n \rightarrow \infty} \hat{\mathbf{I}}_n = \mathbf{I}_0$. Moreover, for any fixed \mathbf{t} and \mathbf{r} , we know that $\lim_{n \rightarrow \infty} R_n(\mathbf{t}, \mathbf{r}) = 0$ (Corollary A.2). Therefore,

$$\lim_{n \rightarrow \infty} \exp \left\{ L_n(\hat{\boldsymbol{\eta}}_n + \mathbf{t}/\sqrt{n}, \hat{\boldsymbol{\zeta}}_n + \mathbf{r}/\sqrt{n}) - L_n(\hat{\boldsymbol{\eta}}_n, \hat{\boldsymbol{\zeta}}_n) \right\} \\ = \exp \left\{ -\frac{1}{2} [\frac{\mathbf{t}}{\mathbf{r}}]^\top \mathbf{I}_0 [\frac{\mathbf{t}}{\mathbf{r}}] \right\} = \exp \left\{ -\frac{1}{2} \mathbf{t}^\top \mathbf{I}_0^{11} \mathbf{t} - \frac{1}{2} \mathbf{r}^\top \mathbf{I}_0^{22} \mathbf{r} - \mathbf{t}^\top \mathbf{I}_0^{12} \mathbf{r} \right\}, \quad (20)$$

where $\mathbf{I}_0 = \begin{bmatrix} \mathbf{I}_0^{11} & \mathbf{I}_0^{12} \\ \mathbf{I}_0^{21} & \mathbf{I}_0^{22} \end{bmatrix}$. Moreover, since $\pi(\boldsymbol{\eta} | \boldsymbol{\zeta})$ is positive and continuous at $\boldsymbol{\eta} = \boldsymbol{\eta}_0$ and $\boldsymbol{\zeta} = \boldsymbol{\zeta}_0$,

$$\lim_{n \rightarrow \infty} g_n(\mathbf{t}, \mathbf{r}) \mathbb{1}\{\mathbf{t} \in B_{n,1}(\delta_t)\} \\ = \exp \left\{ -\frac{1}{2} \mathbf{t}^\top \mathbf{I}_0^{11} \mathbf{t} - \frac{1}{2} \mathbf{r}^\top \mathbf{I}_0^{22} \mathbf{r} - \mathbf{t}^\top \mathbf{I}_0^{12} \mathbf{r} \right\} \pi(\boldsymbol{\eta}_0 | \boldsymbol{\zeta}_0). \quad (21)$$

From (20), we could find $N_{12} \in \mathbb{N}_1$ such that $\forall n > N_{12}$,

$$\exp \left\{ L_n(\hat{\boldsymbol{\eta}}_n + \mathbf{t}/\sqrt{n}, \hat{\boldsymbol{\zeta}}_n + \mathbf{r}/\sqrt{n}) - L_n(\hat{\boldsymbol{\eta}}_n, \hat{\boldsymbol{\zeta}}_n) \right\} < \exp \left\{ -\frac{1}{4} [\frac{\mathbf{t}}{\mathbf{r}}]^\top \mathbf{I}_0 [\frac{\mathbf{t}}{\mathbf{r}}] \right\} \quad (22)$$

Let $N_1 = \max\{N_{11}, N_{12}\}$. Combining (19) and (22) we have, $\forall \mathbf{t} \in B_{n,1}(\delta_t)$, $\forall \mathbf{r} \in A_{n,1}(\delta_r)$ and $\forall n > N_1$,

$$\exp \left\{ L_n(\hat{\boldsymbol{\eta}}_n + \mathbf{t}/\sqrt{n}, \hat{\boldsymbol{\zeta}}_n + \mathbf{r}/\sqrt{n}) - L_n(\hat{\boldsymbol{\eta}}_n, \hat{\boldsymbol{\zeta}}_n) \right\} < \exp \left\{ -\frac{1}{8} \begin{bmatrix} \mathbf{t} \\ \mathbf{r} \end{bmatrix}^\top \mathbf{I}_0 \begin{bmatrix} \mathbf{t} \\ \mathbf{r} \end{bmatrix} \right\}$$

Let $b(\delta_t, \delta_r) = \sup_{\|\boldsymbol{\eta} - \boldsymbol{\eta}_0\| < 2\delta_t, \|\boldsymbol{\zeta} - \boldsymbol{\zeta}_0\| < 2\delta_r} \pi(\boldsymbol{\eta}|\boldsymbol{\zeta})$. Given that $\pi(\boldsymbol{\eta}|\boldsymbol{\zeta})$ is positive and continuous at $\boldsymbol{\eta} = \boldsymbol{\eta}_0$ and $\boldsymbol{\zeta} = \boldsymbol{\zeta}_0$, we can choose δ_r and δ_t small enough so that $b(\delta_t, \delta_r) > 0$. Then $g_n(\mathbf{t}, \mathbf{r}) \mathbb{1}\{\mathbf{t} \in B_{n,1}(\delta_t)\}$ is bounded by

$$b(\delta_t, \delta_r) \int_{B_{n,1}(\delta_t)} \exp \left\{ -\frac{1}{8} \begin{bmatrix} \mathbf{t} \\ \mathbf{r} \end{bmatrix}^\top \mathbf{I}_0 \begin{bmatrix} \mathbf{t} \\ \mathbf{r} \end{bmatrix} \right\} d\mathbf{t},$$

which is clearly integrable. Applying DCT,

$$\begin{aligned} & \lim_{n \rightarrow \infty} \int g_n(\mathbf{t}, \mathbf{r}) \mathbb{1}\{\mathbf{t} \in B_{n,1}(\delta_t)\} d\mathbf{t} \\ &= \int \exp \left\{ -\frac{1}{2} \mathbf{t}^\top \mathbf{I}_0^{11} \mathbf{t} - \frac{1}{2} \mathbf{r}^\top \mathbf{I}_0^{22} \mathbf{r} - \mathbf{t}^\top \mathbf{I}_0^{12} \mathbf{r} \right\} \pi(\boldsymbol{\eta}_0|\boldsymbol{\zeta}_0) d\mathbf{t} \\ &= \exp \left\{ -\frac{1}{2} \mathbf{r}^\top \left(\mathbf{I}_0^{22} - \mathbf{I}_0^{21} (\mathbf{I}_0^{11})^{-1} \mathbf{I}_0^{12} \right) \mathbf{r} \right\} \pi(\boldsymbol{\eta}_0|\boldsymbol{\zeta}_0) |\mathbf{I}_0^{11}| / 2\pi^{-1/2} \end{aligned}$$

We complete the this step by finding the limit for $\int g_n(\mathbf{t}, \mathbf{r}) \mathbb{1}\{\mathbf{t} \in B_{n,2}(\delta_t)\} d\mathbf{t}$. Similar to Step 3 in the proof of Theorem 3.3, we can find $\epsilon > 0$ and $N_2 \in \mathbb{N}_1$ such that $\forall n > N_2$,

$$\frac{1}{n} \left[L_n(\hat{\boldsymbol{\eta}}_n + \mathbf{t}/\sqrt{n}, \hat{\boldsymbol{\zeta}}_n + \mathbf{r}/\sqrt{n}) - L_n(\hat{\boldsymbol{\eta}}_n, \hat{\boldsymbol{\zeta}}_n) \right] < -\epsilon.$$

This implies

$$\begin{aligned} & \lim_{n \rightarrow \infty} \int g_n(\mathbf{t}, \mathbf{r}) \mathbb{1}\{\mathbf{t} \in B_{n,2}(\delta_t)\} d\mathbf{t} \\ & \leq \lim_{n \rightarrow \infty} \exp \{ -n\epsilon \} \int \pi(\hat{\boldsymbol{\eta}}_n + \mathbf{t}/\sqrt{n} | \hat{\boldsymbol{\zeta}}_n + \mathbf{r}/\sqrt{n}) \mathbb{1}\{\mathbf{t} \in B_{n,2}(\delta_t)\} d\mathbf{t} \\ & \leq \lim_{n \rightarrow \infty} \exp \{ -n\epsilon \} \\ & = 0. \end{aligned}$$

Hence we have shown that $\forall \mathbf{r} \in A_{n,2}(\delta_r)$,

$$\lim_{n \rightarrow \infty} a_n(\mathbf{r}) = \exp \left\{ -\frac{1}{2} \mathbf{r}^\top \left(\mathbf{I}_0^{22} - \mathbf{I}_0^{21} (\mathbf{I}_0^{11})^{-1} \mathbf{I}_0^{12} \right) \mathbf{r} \right\} \pi(\boldsymbol{\eta}_0 | \boldsymbol{\zeta}_0) |\mathbf{I}_0^{11} / 2\pi|^{-1/2} \quad (23)$$

Step 2 In this step we will find the limit for $\pi_n^*(\mathbf{t} | \mathbf{r}) \mathbb{1}\{\mathbf{r} \in A_{n,1}(\delta_r)\} \mathbb{1}\{\mathbf{t} \in B_{n,1}(\delta_t)\}$. Since

$$\pi_n^*(\mathbf{t} | \mathbf{r}) \mathbb{1}\{\mathbf{r} \in A_{n,1}(\delta_r)\} \mathbb{1}\{\mathbf{t} \in B_{n,1}(\delta_t)\} = a_n(\mathbf{r})^{-1} g_n(\mathbf{t}, \mathbf{r}) \mathbb{1}\{\mathbf{t} \in B_{n,1}(\delta_t)\},$$

combining (21) and (23) we immediately have

$$\begin{aligned} & \lim_{n \rightarrow \infty} \pi_n^*(\mathbf{t} | \mathbf{r}) \mathbb{1}\{\mathbf{r} \in A_{n,1}(\delta_r)\} \mathbb{1}\{\mathbf{t} \in B_{n,1}(\delta_t)\} \\ &= \lim_{n \rightarrow \infty} a_n(\mathbf{r}) \lim_{n \rightarrow \infty} g_n(\mathbf{t}, \mathbf{r}) \mathbb{1}\{\mathbf{t} \in B_{n,1}(\delta_t)\} \\ &= |\mathbf{I}_0^{11} / 2\pi|^{1/2} \exp \left\{ -\frac{1}{2} \left[\mathbf{t} - (\mathbf{I}_0^{11})^{-1} \mathbf{I}_0^{12} \mathbf{r} \right]^\top \mathbf{I}_0^{11} \left[\mathbf{t} - (\mathbf{I}_0^{11})^{-1} \mathbf{I}_0^{12} \mathbf{r} \right] \right\} \\ &= \phi \left(\mathbf{t} \mid -(\mathbf{I}_0^{11})^{-1} \mathbf{I}_0^{12} \mathbf{r}, (\mathbf{I}_0^{11})^{-1} \right). \end{aligned}$$

Step 3 In this step, we complete the proof by finding a lower bound for $a_n(\mathbf{r})$. Applying Corollary A.2 one more time, by choosing δ_t and δ_r small enough, $\exists N_{31} \in \mathbb{N}_1$ such that $\forall \mathbf{t} \in B_{n,1}(\delta_t)$, $\forall \mathbf{r} \in A_{n,1}(\delta_r)$ and $\forall n > N_{21}$,

$$|R_n(\mathbf{t}, \mathbf{r})| < \frac{1}{4} \begin{bmatrix} \mathbf{t} \\ \mathbf{r} \end{bmatrix}^\top \mathbf{I}_0 \begin{bmatrix} \mathbf{t} \\ \mathbf{r} \end{bmatrix}. \quad (24)$$

Also from (20), $\exists N_{32} \in \mathbb{N}_1$ such that $\forall n > N_{22}$,

$$\begin{aligned} & \exp \left\{ L_n(\hat{\boldsymbol{\eta}}_n + \mathbf{t}/\sqrt{n}, \hat{\boldsymbol{\zeta}}_n + \mathbf{r}/\sqrt{n}) - L_n(\hat{\boldsymbol{\eta}}_n, \hat{\boldsymbol{\zeta}}_n) \right\} \\ & > \exp \left\{ -\frac{1}{2} \begin{bmatrix} \mathbf{t} \\ \mathbf{r} \end{bmatrix}^\top \left(\mathbf{I}_0 + \frac{1}{2} \mathbf{I}_0 \right) \begin{bmatrix} \mathbf{t} \\ \mathbf{r} \end{bmatrix} \right\}. \end{aligned}$$

Combining above and (24), we immediately have that $\forall \mathbf{r} \in A_{n,1}(\delta_r)$, $\forall \mathbf{t} \in B_{n,1}(\delta_t)$ and $\forall n > \max\{N_{31}, N_{32}\}$,

$$\exp \left\{ L_n(\hat{\boldsymbol{\eta}}_n + \mathbf{t}/\sqrt{n}, \hat{\boldsymbol{\zeta}}_n + \mathbf{r}/\sqrt{n}) - L_n(\hat{\boldsymbol{\eta}}_n, \hat{\boldsymbol{\zeta}}_n) \right\} > \exp \left\{ -\begin{bmatrix} \mathbf{t} \\ \mathbf{r} \end{bmatrix}^\top \mathbf{I}_0 \begin{bmatrix} \mathbf{t} \\ \mathbf{r} \end{bmatrix} \right\}. \quad (25)$$

Let $c(\delta_r, \delta_t) = \inf_{\|\boldsymbol{\eta} - \boldsymbol{\eta}_0\| < 2\delta_t, \|\boldsymbol{\zeta} - \boldsymbol{\zeta}_0\| < 2\delta_r} \pi(\boldsymbol{\eta}|\boldsymbol{\zeta})$. Given that $\pi(\boldsymbol{\eta}|\boldsymbol{\zeta})$ is positive and continuous at $\boldsymbol{\eta} = \boldsymbol{\eta}_0$ and $\boldsymbol{\zeta} = \boldsymbol{\zeta}_0$, we can choose δ_r and δ_t small enough so that $c(\delta_r, \delta_t) > 0$. Since $\lim_{n \rightarrow \infty} \hat{\boldsymbol{\eta}}_n = \boldsymbol{\eta}_0$ and $\lim_{n \rightarrow \infty} \hat{\boldsymbol{\zeta}}_n = \boldsymbol{\zeta}_0$, there $\exists N_{33} \in \mathbb{N}_1$ such that $\forall \mathbf{r} \in A_{n,1}(\delta_r)$ and $\forall \mathbf{t} \in B_{n,1}(\delta_t)$, $\pi(\hat{\boldsymbol{\eta}}_n + \mathbf{t}/\sqrt{n}|\hat{\boldsymbol{\zeta}}_n + \mathbf{r}/\sqrt{n}) > c(\delta_r, \delta_t)$. Letting $N_3 = \max\{N_{31}, N_{32}, N_{33}\}$, together with (25), we have shown that $\forall n > N_3$, $a_n(\mathbf{r})$ is lower-bounded by

$$\begin{aligned} & c(\delta_r, \delta_t) \int \exp \left\{ - \begin{bmatrix} \mathbf{t} \\ \mathbf{r} \end{bmatrix}^\top \mathbf{I}_0 \begin{bmatrix} \mathbf{t} \\ \mathbf{r} \end{bmatrix} \right\} d\mathbf{t} \\ & = c(\delta_r, \delta_t) |4\pi \mathbf{I}_0^{11}|^{\frac{1}{2}} \exp \left\{ - \mathbf{r}^\top \left(\mathbf{I}_0^{22} - \mathbf{I}_0^{21} (\mathbf{I}_0^{11})^{-1} \mathbf{I}_0^{12} \right) \mathbf{r} \right\}. \end{aligned} \quad (26)$$

Step 4 Consider $\delta_t > 0$. Since $\lim_{n \rightarrow \infty} \hat{\boldsymbol{\eta}}_n = \boldsymbol{\eta}_0$ (condition 5), for $\forall \mathbf{t} \in B_{n,2}(\delta_t)$ and $\forall \mathbf{r} \in A_{n,1}(\delta_r)$, $\exists N_1 \in \mathbb{N}_1$ such that $\forall n > N_1$,

$$\left\| \begin{bmatrix} \hat{\boldsymbol{\eta}}_n + \mathbf{t}/\sqrt{n} - \boldsymbol{\eta}_0 \\ \hat{\boldsymbol{\zeta}}_n + \mathbf{r}/\sqrt{n} - \boldsymbol{\zeta}_0 \end{bmatrix} \right\| > \|\hat{\boldsymbol{\eta}}_n + \mathbf{t}/\sqrt{n} - \boldsymbol{\eta}_0\| > \frac{\delta_t}{2}.$$

Applying condition 4, $\exists \epsilon > 0$ and $N_2 \geq N_1$ such that $\forall \mathbf{t} \in B_{n,2}(\delta_t)$, $\forall \mathbf{r} \in A_{n,1}(\delta_r)$ and $\forall n > N_2$,

$$\frac{1}{n} [L_n(\hat{\boldsymbol{\eta}}_n + \mathbf{t}/\sqrt{n}, \hat{\boldsymbol{\zeta}}_n + \mathbf{r}/\sqrt{n}) - L_n(\boldsymbol{\eta}_0, \boldsymbol{\zeta}_0)] < -3\epsilon. \quad (27)$$

From condition 2, $\exists N_3 \in \mathbb{N}_1$ such that $\forall n > N_3$, $[\hat{\boldsymbol{\eta}}_n, \hat{\boldsymbol{\zeta}}_n] \in \mathcal{B}_{\mathbf{z}}(\mathbf{z}_0, \delta)$ where $\ell_2(\boldsymbol{\eta}, \boldsymbol{\zeta}, \mathbf{y})$ is thrice differentiable with respect to $\boldsymbol{\eta}$ and $\boldsymbol{\zeta}$. Applying mean value theorem, we have $\frac{1}{n} [L_n(\hat{\boldsymbol{\eta}}_n, \hat{\boldsymbol{\zeta}}_n) - L_n(\boldsymbol{\eta}_0, \boldsymbol{\zeta}_0)] = \frac{1}{n} L_n^{(1)}(\boldsymbol{\eta}'_n, \boldsymbol{\zeta}'_n)^\top [\hat{\boldsymbol{\eta}}_n - \boldsymbol{\eta}_0, \hat{\boldsymbol{\zeta}}_n - \boldsymbol{\zeta}_0]$, where $\boldsymbol{\eta}'_n$ is between $\hat{\boldsymbol{\eta}}_n$ and $\boldsymbol{\eta}_0$ and $\boldsymbol{\zeta}'_n$ is between $\hat{\boldsymbol{\zeta}}_n$ and $\boldsymbol{\zeta}_0$. Using condition 3 and continuous mapping theorem, it can be shown that $\lim_{n \rightarrow \infty} \frac{1}{n} L_n^{(1)}(\boldsymbol{\eta}'_n, \boldsymbol{\zeta}'_n) = \mathbf{0}$. Hence, $\exists N_4 > N_3$ such that $\forall n > N_4$, $\frac{1}{n} |L_n(\hat{\boldsymbol{\eta}}_n, \hat{\boldsymbol{\zeta}}_n) - L_n(\boldsymbol{\eta}_0, \boldsymbol{\zeta}_0)| < \epsilon$. Letting $N = \max\{N_1, \dots, N_4\}$ and using (27), it can be shown that $\forall n > N$,

$$\frac{1}{n} [L_n(\hat{\boldsymbol{\eta}}_n + \mathbf{t}/\sqrt{n}, \hat{\boldsymbol{\zeta}}_n + \mathbf{r}/\sqrt{n}) - L_n(\hat{\boldsymbol{\eta}}_n, \hat{\boldsymbol{\zeta}}_n)] < -2\epsilon. \quad (28)$$

Using Lemma A.3, we can choose δ_t and δ_r to be small enough so that $a_n(\mathbf{r}) \mathbb{1}\{\mathbf{r} \in A_{n,1}(\delta_r)\}$ is lower bounded by (26). Since $\mathbf{I}_0^{22} - \mathbf{I}_0^{21} (\mathbf{I}_0^{11})^{-1} \mathbf{I}_0^{12}$ is positive definite, we can always choose δ_r small enough so that

$$\exp \left\{ - \mathbf{r}^\top \left(\mathbf{I}_0^{22} - \mathbf{I}_0^{21} (\mathbf{I}_0^{11})^{-1} \mathbf{I}_0^{12} \right) \mathbf{r} \right\} < \exp\{n\epsilon\}. \quad (29)$$

Combining (26), (28) and (29), it can be shown that

$$pi_{n,2}^*(\mathbf{t}|\mathbf{r})\mathbb{1}\{\mathbf{r} \in A_{n,1}(\delta_r), \mathbf{t} \in B_{n,1}(\delta_t)\} < \frac{|4\pi\mathbf{I}_0^{11}|^{-1/2}}{c(\delta_r, \delta_t)} \exp\{-n\epsilon\}.$$

□

A.4 Proof of Theorem 3.3

We prove the theorem in the following four steps.

Step 1 Consider $\mathbf{r} = \sqrt{n}(\boldsymbol{\zeta} - \hat{\boldsymbol{\zeta}}_n)$ and its posterior density $\pi_{n,1}^*(\mathbf{r})$. Applying Lemma 3.2 and a simple change of variable, we can show

$$\lim_{n \rightarrow \infty} \int |\pi_{n,1}^*(\mathbf{r}) - \phi(\mathbf{r}|\boldsymbol{\mu}_n, \tilde{\mathbf{I}}_0^{-1})| d\mathbf{r} = 0. \quad (30)$$

It can show that the integral in (9) is bounded by

$$\begin{aligned} & \int \int \pi_{n,2}^*(\mathbf{t}|\mathbf{r}) |\pi_{n,1}^*(\mathbf{r}) - \phi(\mathbf{r}|\boldsymbol{\mu}_n, \tilde{\mathbf{I}}_0^{-1})| d\mathbf{r} d\mathbf{t} \\ & + \int \int \left| \pi_{n,2}^*(\mathbf{t}|\mathbf{r}) - \phi\left(\mathbf{t} \mid -(\mathbf{I}_0^{11})^{-1} \mathbf{I}_0^{12} \mathbf{r}, (\mathbf{I}_0^{11})^{-1}\right) \right| \phi(\mathbf{r}|\boldsymbol{\mu}_n, \tilde{\mathbf{I}}_0^{-1}) d\mathbf{r} d\mathbf{t}, \end{aligned}$$

where the first integral equals $\int |\pi_{n,1}^*(\mathbf{r}) - \phi(\mathbf{r}|\boldsymbol{\mu}_n, \tilde{\mathbf{I}}_0^{-1})| d\mathbf{r}$ which goes to zero by (30). Hence showing

$$\lim_{n \rightarrow \infty} \int \int \left| \pi_{n,2}^*(\mathbf{t}|\mathbf{r}) - \phi\left(\mathbf{t} \mid -(\mathbf{I}_0^{11})^{-1} \mathbf{I}_0^{12} \mathbf{r}, (\mathbf{I}_0^{11})^{-1}\right) \right| \phi(\mathbf{r}|\boldsymbol{\mu}_n, \tilde{\mathbf{I}}_0^{-1}) d\mathbf{r} d\mathbf{t} = 0 \quad (31)$$

would be enough for proving (9).

Step 2 For $\delta_r > 0$, the integral in (31) can be written as

$$\begin{aligned} & \int \int_{\mathbf{r} \in A_{n,1}(\delta_r)} \left| \pi_{n,2}^*(\mathbf{t}|\mathbf{r}) - \phi\left(\mathbf{t} \mid -(\mathbf{I}_0^{11})^{-1} \mathbf{I}_0^{12} \mathbf{r}, (\mathbf{I}_0^{11})^{-1}\right) \right| \phi(\mathbf{r}|\boldsymbol{\mu}_n, \tilde{\mathbf{I}}_0^{-1}) d\mathbf{r} d\mathbf{t} \\ & + \int \int_{\mathbf{r} \in A_{n,2}(\delta_r)} \left| \pi_{n,2}^*(\mathbf{t}|\mathbf{r}) - \phi\left(\mathbf{t} \mid -(\mathbf{I}_0^{11})^{-1} \mathbf{I}_0^{12} \mathbf{r}, (\mathbf{I}_0^{11})^{-1}\right) \right| \phi(\mathbf{r}|\boldsymbol{\mu}_n, \tilde{\mathbf{I}}_0^{-1}) d\mathbf{r} d\mathbf{t}, \end{aligned}$$

where the second integral is clearly bounded by

$$\begin{aligned} & \int_{\mathbf{r} \in A_{n,2}(\delta_r)} \int \left| \pi_{n,2}^*(\mathbf{t}|\mathbf{r}) - \phi\left(\mathbf{t} \mid -(\mathbf{I}_0^{11})^{-1} \mathbf{I}_0^{12} \mathbf{r}, (\mathbf{I}_0^{11})^{-1}\right) \right| dt \phi(\mathbf{r}|\boldsymbol{\mu}_n, \tilde{\mathbf{I}}_0^{-1}) d\mathbf{r} \\ & \leq 2 \int_{\mathbf{r} \in A_{n,2}(\delta_r)} \phi(\mathbf{r}|\boldsymbol{\mu}_n, \tilde{\mathbf{I}}_0^{-1}) d\mathbf{r} \end{aligned}$$

Transforming \mathbf{r} back to ζ ,

$$\int_{\mathbf{r} \in A_{n,2}(\delta_r)} \phi(\mathbf{r} | \boldsymbol{\mu}_n, \tilde{\mathbf{I}}^{-1}) d\mathbf{r} = \Phi \left(\|\zeta - \zeta_0\| > \delta_r \middle| \tilde{\zeta}_n, \tilde{\mathbf{I}}_0/n \right).$$

From condition 5, $\lim_{n \rightarrow \infty} \hat{\zeta}_n = \zeta_0$ and hence by continuous mapping theorem,

$$\lim_{n \rightarrow \infty} \Phi \left(\|\zeta - \zeta_0\| > \delta_r \middle| \tilde{\zeta}_n, \tilde{\mathbf{I}}_0/n \right) = \lim_{n \rightarrow \infty} \Phi \left(\|\zeta - \zeta_0\| > \delta_r \middle| \zeta_0, \tilde{\mathbf{I}}_0/n \right) = 0.$$

This implies that showing

$$\int \int_{\mathbf{r} \in A_{n,1}(\delta_r)} \left| \pi_{n,2}^*(\mathbf{t} | \mathbf{r}) - \phi \left(\mathbf{t} \middle| -(\mathbf{I}_0^{11})^{-1} \mathbf{I}_0^{12} \mathbf{r}, (\mathbf{I}_0^{11})^{-1} \right) \right| \phi(\mathbf{r} | \boldsymbol{\mu}_n, \tilde{\mathbf{I}}^{-1}) d\mathbf{r} d\mathbf{t} \rightarrow 0 \quad (32)$$

would be enough for proving (31).

Step 3 Applying (17) in Lemma A.3, we have

$$\int_{\mathbf{t} \in B_{n,2}(\delta_t)} \int_{\mathbf{r} \in A_{n,1}(\delta_r)} \pi_{n,2}^*(\mathbf{t} | \mathbf{r}) \phi(\mathbf{r} | \boldsymbol{\mu}_n, \tilde{\mathbf{I}}_0^{-1}) d\mathbf{r} d\mathbf{t} < \frac{|4\pi \mathbf{I}_0^{11}|^{-1/2}}{c(\delta_r, \delta_t)} \exp\{-n\epsilon\} \rightarrow 0.$$

Moreover, it can be easily shown that

$$\int_{\mathbf{t} \in B_{n,2}(\delta_t)} \int_{\mathbf{r} \in A_{n,1}(\delta_r)} \phi \left(\mathbf{t} \middle| -(\mathbf{I}_0^{11})^{-1} \mathbf{I}_0^{12} \mathbf{r}, (\mathbf{I}_0^{11})^{-1} \right) \phi(\mathbf{r} | \boldsymbol{\mu}_n, \tilde{\mathbf{I}}_0^{-1}) d\mathbf{r} d\mathbf{t} \rightarrow 0.$$

Hence we have shown that

$$\begin{aligned} & \lim_{n \rightarrow \infty} \int_{\mathbf{t} \in B_{n,2}(\delta_t)} \int_{\mathbf{r} \in A_{n,1}(\delta_r)} \left| \pi_{n,2}^*(\mathbf{t} | \mathbf{r}) - \phi \left(\mathbf{t} \middle| -(\mathbf{I}_0^{11})^{-1} \mathbf{I}_0^{12} \mathbf{r}, (\mathbf{I}_0^{11})^{-1} \right) \right| \\ & \quad \times \phi(\mathbf{r} | \boldsymbol{\mu}_n, \tilde{\mathbf{I}}^{-1}) d\mathbf{r} d\mathbf{t} = 0. \end{aligned}$$

This implies that showing

$$\begin{aligned} & \lim_{n \rightarrow \infty} \int_{\mathbf{t} \in B_{n,1}(\delta_t)} \int_{\mathbf{r} \in A_{n,1}(\delta_r)} \left| \pi_{n,2}^*(\mathbf{t} | \mathbf{r}) - \phi \left(\mathbf{t} \middle| -(\mathbf{I}_0^{11})^{-1} \mathbf{I}_0^{12} \mathbf{r}, (\mathbf{I}_0^{11})^{-1} \right) \right| \\ & \quad \times \phi(\mathbf{r} | \boldsymbol{\mu}_n, \tilde{\mathbf{I}}_0^{-1}) d\mathbf{r} d\mathbf{t} = 0 \end{aligned} \quad (33)$$

would be enough for proving (32).

Step 4 Since $\phi(\mathbf{r}|\boldsymbol{\mu}_n, \tilde{\mathbf{I}}_0^{-1})$ is bounded by $|\tilde{\mathbf{I}}/2\pi|^{1/2}$, applying (16) in Lemma A.3 again we have

$$\begin{aligned} & \lim_{n \rightarrow \infty} \left| \pi_{n,2}^*(\mathbf{t}|\mathbf{r}) - \phi\left(\mathbf{t} \middle| -(\mathbf{I}_0^{11})^{-1} \mathbf{I}_0^{12} \mathbf{r}, (\mathbf{I}_0^{11})^{-1}\right) \right| \\ & \quad \times \phi(\mathbf{r}|\boldsymbol{\mu}_n, \tilde{\mathbf{I}}_0^{-1}) \mathbb{1}_{\mathbf{t} \in B_{n,1}(\delta_t)} \mathbb{1}_{\mathbf{r} \in A_{n,1}(\delta_r)} = 0. \end{aligned}$$

Moreover,

$$\begin{aligned} & \int_{\mathbf{t} \in B_{n,1}(\delta_t)} \int_{\mathbf{r} \in A_{n,1}(\delta_r)} \left| \pi_{n,2}^*(\mathbf{t}|\mathbf{r}) - \phi\left(\mathbf{t} \middle| -(\mathbf{I}_0^{11})^{-1} \mathbf{I}_0^{12} \mathbf{r}, (\mathbf{I}_0^{11})^{-1}\right) \right| \\ & \quad \times \phi(\mathbf{r}|\boldsymbol{\mu}_n, \tilde{\mathbf{I}}_0^{-1}) d\mathbf{r} d\mathbf{t} \\ & < \int_{\mathbf{t} \in B_{n,1}(\delta_t)} \int_{\mathbf{r} \in A_{n,1}(\delta_r)} \phi\left(\mathbf{t} \middle| -(\mathbf{I}_0^{11})^{-1} \mathbf{I}_0^{12} \mathbf{r}, (\mathbf{I}_0^{11})^{-1}\right) \phi(\mathbf{r}|\boldsymbol{\mu}_n, \tilde{\mathbf{I}}_0^{-1}) d\mathbf{r} d\mathbf{t} \\ & \quad + \int_{\mathbf{t} \in B_{n,1}(\delta_t)} \int_{\mathbf{r} \in A_{n,1}(\delta_r)} \pi_{n,2}^*(\mathbf{t}|\mathbf{r}) \phi(\mathbf{r}|\boldsymbol{\mu}_n, \tilde{\mathbf{I}}_0^{-1}) d\mathbf{r} d\mathbf{t} \\ & \leq 2. \end{aligned}$$

Therefore by Scheffé's lemma we have shown (33).

A.5 Proof of Lemma A.4

We now provide a lemma that will be needed in our later proof of Corollary 3.4. It characterizes the asymptotic difference between $\tilde{\boldsymbol{\zeta}}_n$ and $\hat{\boldsymbol{\zeta}}_n$.

Lemma A.4. *Suppose that the conditions for Theorem 3.3 hold, then*

$$\sqrt{n}(\tilde{\boldsymbol{\zeta}}_n - \hat{\boldsymbol{\zeta}}_n) \xrightarrow{d} \mathcal{N}(\mathbf{0}, \mathbf{V}),$$

where \mathbf{V} is a positive definite matrix.

Proof. Expanding Taylor series for $\frac{1}{n}L_n^{(1)}(\hat{\boldsymbol{\eta}}_n, \hat{\boldsymbol{\zeta}}_n)$ we have

$$\mathbf{0} = \frac{1}{n}L_n^{(1)}(\hat{\boldsymbol{\eta}}_n, \hat{\boldsymbol{\zeta}}_n) = \frac{1}{n}L_n^{(1)}(\boldsymbol{\eta}_0, \boldsymbol{\zeta}_0) + \frac{1}{n}L_n^{(2)}(\boldsymbol{\eta}'_n, \boldsymbol{\zeta}'_n) \begin{bmatrix} \hat{\boldsymbol{\eta}}_n - \boldsymbol{\eta}_0 \\ \hat{\boldsymbol{\zeta}}_n - \boldsymbol{\zeta}_0 \end{bmatrix},$$

where $\boldsymbol{\eta}'_n$ is between $\boldsymbol{\eta}_0$ and $\hat{\boldsymbol{\eta}}_n$ and $\boldsymbol{\zeta}'_n$ is between $\boldsymbol{\zeta}_0$ and $\hat{\boldsymbol{\zeta}}_n$. Letting $\hat{\mathbf{I}}_n = \frac{1}{n}L_n^{(2)}(\boldsymbol{\eta}'_n, \boldsymbol{\zeta}'_n)$, we have

$$\begin{bmatrix} \sqrt{n}(\hat{\boldsymbol{\eta}}_n - \boldsymbol{\eta}_0) \\ \sqrt{n}(\hat{\boldsymbol{\zeta}}_n - \boldsymbol{\zeta}_0) \end{bmatrix} = -\hat{\mathbf{I}}_n^{-1} \sqrt{n} \frac{1}{n} L_n^{(1)}(\boldsymbol{\eta}_0, \boldsymbol{\zeta}_0). \quad (34)$$

Since condition 5 holds for $f_2(\mathbf{y}|\boldsymbol{\eta}, \boldsymbol{\zeta})$, we know that $\lim_{n \rightarrow \infty} \hat{\boldsymbol{\eta}}_n = \boldsymbol{\eta}_0$ and $\lim_{n \rightarrow \infty} \hat{\boldsymbol{\zeta}}_n = \boldsymbol{\zeta}_0$. Applying continuous mapping theorem and condition 3, we have that $\lim_{n \rightarrow \infty} \hat{\mathbf{I}}_n = \mathbf{I}_0$. Letting \mathbf{D}_1 denote a $(d_\eta + d_\zeta)$ -dimensional identity matrix, we can rewrite (34) as

$$\begin{aligned} \begin{bmatrix} \sqrt{n}(\hat{\boldsymbol{\eta}}_n - \boldsymbol{\eta}_0) \\ \sqrt{n}(\hat{\boldsymbol{\zeta}}_n - \boldsymbol{\zeta}_0) \end{bmatrix} &= -\hat{\mathbf{I}}_n^{-1} \mathbf{I}_0 \sqrt{n} \frac{1}{n} \mathbf{I}_0^{-1} L_n^{(1)}(\boldsymbol{\eta}_0, \boldsymbol{\zeta}_0) \\ &= -(\hat{\mathbf{I}}_n^{-1} \mathbf{I}_0 - \mathbf{D}_1) \sqrt{n} \frac{1}{n} \mathbf{I}_0^{-1} L_n^{(1)}(\boldsymbol{\eta}_0, \boldsymbol{\zeta}_0) - \sqrt{n} \frac{1}{n} \mathbf{I}_0^{-1} L_n^{(1)}(\boldsymbol{\eta}_0, \boldsymbol{\zeta}_0) \end{aligned}$$

Before proceeding, we introduce the following notation. Letting \mathbf{A} be any $(d_\eta + d_\zeta)$ -dimensional square matrix, we let

$$\mathbf{A} = \begin{bmatrix} \text{upper}(\mathbf{A}) \\ \text{lower}(\mathbf{A}) \end{bmatrix},$$

where $\text{upper}(\mathbf{A})$ is a $d_\eta \times (d_\eta + d_\zeta)$ -dimensional matrix and $\text{lower}(\mathbf{A})$ is a $d_\zeta \times (d_\eta + d_\zeta)$ matrix. Using this notation,

$$\begin{aligned} \sqrt{n}(\hat{\boldsymbol{\zeta}}_n - \boldsymbol{\zeta}_0) &= -\text{lower}[(\hat{\mathbf{I}}_n^{-1} \mathbf{I}_0 - \mathbf{D}_1)] \sqrt{n} \frac{1}{n} \mathbf{I}_0^{-1} L_n^{(1)}(\boldsymbol{\eta}_0, \boldsymbol{\zeta}_0) \\ &\quad - \text{lower}(\mathbf{D}_1) \sqrt{n} \frac{1}{n} \mathbf{I}_0^{-1} L_n^{(1)}(\boldsymbol{\eta}_0, \boldsymbol{\zeta}_0) \end{aligned} \quad (35)$$

Expanding Taylor series for $\frac{1}{n} Q_n^{(1)}(\tilde{\boldsymbol{\zeta}}_n)$, we have

$$\mathbf{0} = \frac{1}{n} Q_n^{(1)}(\tilde{\boldsymbol{\zeta}}_n) = \frac{1}{n} Q_n^{(1)}(\boldsymbol{\zeta}_0) + \frac{1}{n} Q_n^{(2)}(\boldsymbol{\zeta}_n^*)(\tilde{\boldsymbol{\zeta}}_n - \boldsymbol{\zeta}_0),$$

where $\boldsymbol{\zeta}_n^*$ is between $\boldsymbol{\zeta}_0$ and $\tilde{\boldsymbol{\zeta}}_n$. Letting $\tilde{\mathbf{I}}_n = \frac{1}{n} Q_n^{(2)}(\boldsymbol{\zeta}_n^*)$, we have

$$\sqrt{n}(\tilde{\boldsymbol{\zeta}}_n - \boldsymbol{\zeta}_0) = -\tilde{\mathbf{I}}_n^{-1} \sqrt{n} \frac{1}{n} Q_n^{(1)}(\boldsymbol{\zeta}_0). \quad (36)$$

Similarly, using the fact that conditions 3, 5 hold for $f_1(\mathbf{y}|\boldsymbol{\zeta})$ and the continuous mapping theorem, we have that $\lim_{n \rightarrow \infty} \tilde{\mathbf{I}}_n = \tilde{\mathbf{I}}_0$. Letting \mathbf{D}_2 denote the d_ζ -dimensional identity matrix, we can rewrite (36) as

$$\begin{aligned} \sqrt{n}(\tilde{\boldsymbol{\zeta}}_n - \boldsymbol{\zeta}_0) &= -\tilde{\mathbf{I}}_n^{-1} \tilde{\mathbf{I}}_0 \sqrt{n} \frac{1}{n} \tilde{\mathbf{I}}_0^{-1} Q_n^{(1)}(\boldsymbol{\zeta}_0) \\ &= -(\tilde{\mathbf{I}}_n^{-1} \tilde{\mathbf{I}}_0 - \mathbf{D}_2) \sqrt{n} \frac{1}{n} \tilde{\mathbf{I}}_0^{-1} Q_n^{(1)}(\boldsymbol{\zeta}_0) - \sqrt{n} \frac{1}{n} \tilde{\mathbf{I}}_0^{-1} Q_n^{(1)}(\boldsymbol{\zeta}_0) \end{aligned}$$

Combining above and (35), we have

$$\begin{aligned} & \sqrt{n}(\tilde{\boldsymbol{\zeta}}_n - \hat{\boldsymbol{\zeta}}_n) \\ = & -(\tilde{\mathbf{I}}_n^{-1}\tilde{\mathbf{I}}_0 - \mathbf{D}_2)\sqrt{n}\frac{1}{n}\tilde{\mathbf{I}}_0^{-1}Q_n^{(1)}(\boldsymbol{\zeta}_0) + \text{lower}[(\hat{\mathbf{I}}_n^{-1}\mathbf{I}_0 - \mathbf{D}_1)]\sqrt{n}\frac{1}{n}\mathbf{I}_0^{-1}L_n^{(1)}(\boldsymbol{\eta}_0, \boldsymbol{\zeta}_0) \\ & - \sqrt{n}\frac{1}{n}\left[\tilde{\mathbf{I}}_0^{-1}Q_n^{(1)}(\boldsymbol{\zeta}_0) - \text{lower}(\mathbf{D}_1)\mathbf{I}_0^{-1}L_n^{(1)}(\boldsymbol{\eta}_0, \boldsymbol{\zeta}_0)\right]. \end{aligned}$$

Since condition 3 holds for $f_1(\mathbf{y}|\boldsymbol{\zeta})$, we know that $\mathbb{E}_{\boldsymbol{\theta}_0}\nabla_{\boldsymbol{\zeta}}\ell_1(\boldsymbol{\zeta}, \mathbf{y})|_{\boldsymbol{\theta}=\boldsymbol{\theta}_0} = \mathbf{0}$, and hence $\text{Var}_{\boldsymbol{\theta}_0}\nabla_{\boldsymbol{\zeta}}\ell_1(\boldsymbol{\zeta}, \mathbf{y})|_{\boldsymbol{\theta}=\boldsymbol{\theta}_0} = \tilde{\mathbf{I}}_0$. Similarly, since condition 3 holds for $f_2(\mathbf{y}|\boldsymbol{\eta}, \boldsymbol{\zeta})$, we know that $\mathbb{E}_{\boldsymbol{\theta}_0}\nabla_{\boldsymbol{\eta}, \boldsymbol{\zeta}}\ell_2(\boldsymbol{\eta}, \boldsymbol{\zeta}, \mathbf{y})|_{\boldsymbol{\theta}=\boldsymbol{\theta}_0} = \mathbf{0}$ and $\text{Var}_{\boldsymbol{\theta}_0}\nabla_{\boldsymbol{\eta}, \boldsymbol{\zeta}}\ell_2(\boldsymbol{\eta}, \boldsymbol{\zeta}, \mathbf{y})|_{\boldsymbol{\theta}=\boldsymbol{\theta}_0} = \mathbf{I}_0$. It is easily seen that

$$\mathbb{E}_{\boldsymbol{\theta}_0}\tilde{\mathbf{I}}_0^{-1}\nabla_{\boldsymbol{\zeta}}\ell_1(\boldsymbol{\zeta}, \mathbf{y})|_{\boldsymbol{\theta}=\boldsymbol{\theta}_0} = \mathbf{0}, \quad \mathbb{E}_{\boldsymbol{\theta}_0}\text{lower}(\mathbf{D}_1)\mathbf{I}_0^{-1}\nabla_{\boldsymbol{\eta}, \boldsymbol{\zeta}}\ell_2(\boldsymbol{\eta}, \boldsymbol{\zeta}, \mathbf{y})|_{\boldsymbol{\theta}=\boldsymbol{\theta}_0} = \mathbf{0}$$

and hence

$$\mathbb{E}_{\boldsymbol{\theta}_0}\left[\tilde{\mathbf{I}}_0^{-1}\nabla_{\boldsymbol{\zeta}}\ell_1(\boldsymbol{\zeta}, \mathbf{y}) - \text{lower}(\mathbf{D}_1)\mathbf{I}_0^{-1}\nabla_{\boldsymbol{\eta}, \boldsymbol{\zeta}}\ell_2(\boldsymbol{\eta}, \boldsymbol{\zeta}, \mathbf{y})\right]\Bigg|_{\boldsymbol{\theta}=\boldsymbol{\theta}_0} = \mathbf{0}.$$

Also, it can be shown that

$$\begin{aligned} \text{Var}_{\boldsymbol{\theta}_0}\tilde{\mathbf{I}}_0^{-1}\nabla_{\boldsymbol{\zeta}}\ell_1(\boldsymbol{\zeta}, \mathbf{y})|_{\boldsymbol{\theta}=\boldsymbol{\theta}_0} &= \tilde{\mathbf{I}}_0^{-1}\tilde{\mathbf{I}}_0\tilde{\mathbf{I}}_0^{-1} = \tilde{\mathbf{I}}_0^{-1}, \\ \text{Var}_{\boldsymbol{\theta}_0}\mathbf{I}_0^{-1}\nabla_{\boldsymbol{\eta}, \boldsymbol{\zeta}}\ell_2(\boldsymbol{\eta}, \boldsymbol{\zeta}, \mathbf{y})|_{\boldsymbol{\theta}=\boldsymbol{\theta}_0} &= \mathbf{I}_0^{-1}\mathbf{I}_0\mathbf{I}_0^{-1} = \mathbf{I}_0^{-1}. \end{aligned}$$

Applying central limit theorem (CLT), we have

$$\sqrt{n}\frac{1}{n}\tilde{\mathbf{I}}_0^{-1}Q_n^{(1)}(\boldsymbol{\zeta}_0) \xrightarrow{d} \mathcal{N}(\mathbf{0}, \tilde{\mathbf{I}}_0^{-1}) \quad (37)$$

$$\sqrt{n}\frac{1}{n}\mathbf{I}_0^{-1}L_n^{(1)}(\boldsymbol{\eta}_0, \boldsymbol{\zeta}_0) \xrightarrow{d} \mathcal{N}(\mathbf{0}, \mathbf{I}_0^{-1}). \quad (38)$$

Introducing

$$\mathbf{V} = \text{Var}_{\boldsymbol{\theta}_0}\left[\tilde{\mathbf{I}}_0^{-1}\nabla_{\boldsymbol{\zeta}}\ell_1(\boldsymbol{\zeta}, \mathbf{y}) - \text{lower}(\mathbf{D}_1)\mathbf{I}_0^{-1}\nabla_{\boldsymbol{\eta}, \boldsymbol{\zeta}}\ell_2(\boldsymbol{\eta}, \boldsymbol{\zeta}, \mathbf{y})\right]\Bigg|_{\boldsymbol{\theta}=\boldsymbol{\theta}_0}$$

and applying CLT again, we have

$$\sqrt{n}\frac{1}{n}\left[\tilde{\mathbf{I}}_0^{-1}Q_n^{(1)}(\boldsymbol{\zeta}_0) - \text{lower}(\mathbf{D}_1)\mathbf{I}_0^{-1}L_n^{(1)}(\boldsymbol{\eta}_0, \boldsymbol{\zeta}_0)\right] \xrightarrow{d} \mathcal{N}(\mathbf{0}, \mathbf{V}).$$

We have already shown that $\lim_{n \rightarrow \infty} \tilde{\mathbf{I}}_n = \tilde{\mathbf{I}}_0$, which implies that $\lim_{n \rightarrow \infty} \tilde{\mathbf{I}}_n^{-1} \tilde{\mathbf{I}}_0 = \mathbf{D}_2$. Similarly, we have shown that $\lim_{n \rightarrow \infty} \hat{\mathbf{I}}_n = \mathbf{I}_0$, which implies $\lim_{n \rightarrow \infty} \hat{\mathbf{I}}_n^{-1} \mathbf{I}_0 = \mathbf{D}_1$. Combining (37) and (38) and applying Slutsky's theorem, we have

$$\begin{aligned} & (\tilde{\mathbf{I}}_n^{-1} \tilde{\mathbf{I}}_0 - \mathbf{D}_2) \sqrt{n} \frac{1}{n} \tilde{\mathbf{I}}_n^{-1} Q_n^{(1)}(\zeta_0) \xrightarrow{d} \mathbf{0}, \\ & \text{lower}[(\hat{\mathbf{I}}_n^{-1} \mathbf{I}_0 - \mathbf{D}_1)] \sqrt{n} \frac{1}{n} \mathbf{I}_0^{-1} L_n^{(1)}(\boldsymbol{\eta}_0, \zeta_0) \xrightarrow{d} \mathbf{0}. \end{aligned}$$

Since convergence in distribution to a constant implies convergence in probability, we have

$$\begin{aligned} & (\tilde{\mathbf{I}}_n^{-1} \tilde{\mathbf{I}}_0 - \mathbf{D}_2) \sqrt{n} \frac{1}{n} \tilde{\mathbf{I}}_n^{-1} Q_n^{(1)}(\zeta_0) \xrightarrow{P_{\theta_0}} \mathbf{0}, \\ & \text{lower}[(\hat{\mathbf{I}}_n^{-1} \mathbf{I}_0 - \mathbf{D}_1)] \sqrt{n} \frac{1}{n} \mathbf{I}_0^{-1} L_n^{(1)}(\boldsymbol{\eta}_0, \zeta_0) \xrightarrow{P_{\theta_0}} \mathbf{0}, \end{aligned}$$

which implies that

$$\sqrt{n}(\tilde{\zeta}_n - \hat{\zeta}_n) \xrightarrow{P_{\theta_0}} -\sqrt{n} \frac{1}{n} \left[\tilde{\mathbf{I}}_0^{-1} Q_n^{(1)}(\zeta_0) - \text{lower}(\mathbf{D}_1) \mathbf{I}_0^{-1} L_n^{(1)}(\boldsymbol{\eta}_0, \zeta_0) \right],$$

where the right part has been shown to converge in distribution to $\mathcal{N}(\mathbf{0}, \mathbf{V})$. Hence we can conclude that

$$\sqrt{n}(\tilde{\zeta}_n - \hat{\zeta}_n) \xrightarrow{d} \mathcal{N}(\mathbf{0}, \mathbf{V}).$$

□

A.6 Proof of Corollary 3.4

Applying random variable transformation to (9), it can be shown that

$$\lim_{n \rightarrow \infty} \int \int |g_n(\boldsymbol{\eta}, \zeta)| d\boldsymbol{\eta} d\zeta = 0,$$

where

$$\begin{aligned} g_n(\boldsymbol{\eta}, \zeta) &= \tau_n(\boldsymbol{\eta} | \zeta) \kappa_n(\zeta) \\ &- \phi\left(\boldsymbol{\eta} \mid \hat{\boldsymbol{\eta}}_n - (\mathbf{I}_0^{11})^{-1} \mathbf{I}_0^{12} (\zeta - \hat{\zeta}_n), (\mathbf{I}_0^{11})^{-1} / \sqrt{n}\right) \phi\left(\zeta \mid \tilde{\zeta}_n, \tilde{\mathbf{I}}_0^{-1} / \sqrt{n}\right). \end{aligned}$$

Let $\mathbf{z} = \begin{bmatrix} \boldsymbol{\eta} \\ \boldsymbol{\zeta} \end{bmatrix}$ and $\mathbf{z}_0 = \begin{bmatrix} \boldsymbol{\eta}_0 \\ \boldsymbol{\zeta}_0 \end{bmatrix}$. For any neighborhood U of \mathbf{z}_0 , $\exists \delta > 0$ such that $B = \mathcal{B}_{\mathbf{z}}(\mathbf{z}_0, \delta) \in U$. Then it can be shown that

$$\begin{aligned}
& \lim_{n \rightarrow \infty} \int_U \tau_n(\boldsymbol{\eta}|\boldsymbol{\zeta}) \kappa_n(\boldsymbol{\zeta}) \, d\boldsymbol{\eta} d\boldsymbol{\zeta} \\
&= \lim_{n \rightarrow \infty} \int_U \phi\left(\boldsymbol{\eta} \middle| \hat{\boldsymbol{\eta}}_n - (\mathbf{I}_0^{11})^{-1} \mathbf{I}_0^{12} (\boldsymbol{\zeta} - \hat{\boldsymbol{\zeta}}_n), (\mathbf{I}_0^{11})^{-1} / \sqrt{n}\right) \phi\left(\boldsymbol{\zeta} \middle| \tilde{\boldsymbol{\zeta}}_n, \tilde{\mathbf{I}}_0^{-1} / \sqrt{n}\right) \, d\boldsymbol{\eta} d\boldsymbol{\zeta} \\
&\quad + \lim_{n \rightarrow \infty} \int_U |g_n(\boldsymbol{\eta}, \boldsymbol{\zeta})| \, d\boldsymbol{\eta} d\boldsymbol{\zeta} \\
&= \lim_{n \rightarrow \infty} \int_U \phi\left(\boldsymbol{\eta} \middle| \hat{\boldsymbol{\eta}}_n - (\mathbf{I}_0^{11})^{-1} \mathbf{I}_0^{12} (\boldsymbol{\zeta} - \hat{\boldsymbol{\zeta}}_n), (\mathbf{I}_0^{11})^{-1} / \sqrt{n}\right) \phi\left(\boldsymbol{\zeta} \middle| \tilde{\boldsymbol{\zeta}}_n, \tilde{\mathbf{I}}_0^{-1} / \sqrt{n}\right) \, d\boldsymbol{\eta} d\boldsymbol{\zeta} \\
&\geq \lim_{n \rightarrow \infty} \int_B \phi\left(\boldsymbol{\eta} \middle| \hat{\boldsymbol{\eta}}_n - (\mathbf{I}_0^{11})^{-1} \mathbf{I}_0^{12} (\boldsymbol{\zeta} - \hat{\boldsymbol{\zeta}}_n), (\mathbf{I}_0^{11})^{-1} / \sqrt{n}\right) \phi\left(\boldsymbol{\zeta} \middle| \tilde{\boldsymbol{\zeta}}_n, \tilde{\mathbf{I}}_0^{-1} / \sqrt{n}\right) \, d\boldsymbol{\eta} d\boldsymbol{\zeta}
\end{aligned}$$

Since condition 5 holds for both $f_1(\mathbf{y}|\boldsymbol{\zeta})$ and $f_2(\mathbf{y}|\boldsymbol{\eta}, \boldsymbol{\zeta})$, we have $\lim_{n \rightarrow \infty} \hat{\boldsymbol{\eta}}_n = \boldsymbol{\eta}_0$, $\lim_{n \rightarrow \infty} \hat{\boldsymbol{\zeta}}_n = \boldsymbol{\zeta}_0$ and $\lim_{n \rightarrow \infty} \tilde{\boldsymbol{\zeta}}_n = \boldsymbol{\zeta}_0$. Hence the above limit goes to 1.

A.7 Proof of Theorem 3.7

Letting $\mathbf{r}_n^* = \sqrt{n} (\boldsymbol{\zeta}_n^* - \hat{\boldsymbol{\zeta}}_n)$, it can be seen that $\pi_{n,3}^*(\mathbf{t}) = \pi_{n,2}^*(\mathbf{t}|\mathbf{r}_n^*)$. Suppose that the conditions for Theorem 3.3 hold, then slightly modifying the step 3 and step 4 in the proof of Theorem 3.3 we can show that $\exists \delta > 0$ such that for $\|\mathbf{r}_n^*\| < \sqrt{n}\delta$,

$$\lim_{n \rightarrow \infty} \int \left| \pi_{n,3}^*(\mathbf{t}) - \phi\left(\mathbf{t} \middle| -(\mathbf{I}_0^{11})^{-1} \mathbf{I}_0^{12} \boldsymbol{\mu}_n, (\mathbf{I}_0^{11})^{-1}\right) \right| \, d\mathbf{t} = 0.$$

Define a sequence of events $A_{n,\delta} = \{\mathbf{r}_n^* : \|\mathbf{r}_n^*\| < \sqrt{n}\delta\}$ and $B_{n,\delta} = \{\mathbf{r}_n^* : \|\mathbf{r}_n^*\| > \sqrt{n}\delta\}$, then for any $\epsilon > 0$, we have

$$\begin{aligned}
& p \left[\int \left| \pi_{n,3}^*(\mathbf{t}) - \phi\left(\mathbf{t} \middle| -(\mathbf{I}_0^{11})^{-1} \mathbf{I}_0^{12} \boldsymbol{\mu}_n, (\mathbf{I}_0^{11})^{-1}\right) \right| \, d\mathbf{t} > \epsilon \right] \\
&= p(A_{n,\delta}) p \left[\int \left| \pi_{n,3}^*(\mathbf{t}) - \phi\left(\mathbf{t} \middle| -(\mathbf{I}_0^{11})^{-1} \mathbf{I}_0^{12} \boldsymbol{\mu}_n, (\mathbf{I}_0^{11})^{-1}\right) \right| \, d\mathbf{t} > \epsilon \middle| A_{n,\delta} \right] \\
&\quad + p(B_{n,\delta}) p \left[\int \left| \pi_{n,3}^*(\mathbf{t}) - \phi\left(\mathbf{t} \middle| -(\mathbf{I}_0^{11})^{-1} \mathbf{I}_0^{12} \boldsymbol{\mu}_n, (\mathbf{I}_0^{11})^{-1}\right) \right| \, d\mathbf{t} > \epsilon \middle| B_{n,\delta} \right]
\end{aligned} \tag{39}$$

We have already shown that

$$\lim_{n \rightarrow \infty} p \left[\int \left| \pi_{n,3}^*(\mathbf{t}) - \phi \left(\mathbf{t} \middle| -(\mathbf{I}_0^{11})^{-1} \mathbf{I}_0^{12} \boldsymbol{\mu}_n, (\mathbf{I}_0^{11})^{-1} \right) \right| d\mathbf{t} > \epsilon \middle| A_{n,\delta} \right] = 0.$$

Since $p(A_{n,1}) \leq 1$, the first part in (39) goes to 0.

Similarly, we also know

$$p \left(\int \left| \pi_{n,3}^*(\mathbf{t}) - \phi \left(\mathbf{t} \middle| -(\mathbf{I}_0^{11})^{-1} \mathbf{I}_0^{12} \boldsymbol{\mu}_n, (\mathbf{I}_0^{11})^{-1} \right) \right| d\mathbf{t} > \epsilon \middle| A_{n,2} \right) \leq 1.$$

From Lemma 3.6, we know that $\lim_{n \rightarrow \infty} \sqrt{n} (\boldsymbol{\zeta}_n^* - \tilde{\boldsymbol{\zeta}}_n) = 0$. From Lemma A.4, we know that $\sqrt{n} (\tilde{\boldsymbol{\zeta}}_n - \hat{\boldsymbol{\zeta}}_n) \xrightarrow{d} \mathcal{N}(\mathbf{0}, \mathbf{V})$. Combining them we can show that $\mathbf{r}_n^* \xrightarrow{d} \mathcal{N}(\mathbf{0}, \mathbf{V})$, hence

$$p(B_{n,\delta}) = p(\|\mathbf{r}_n^*\| > \sqrt{n}\delta)$$

also goes to zero. We have shown that the second part in (39) goes to 0.

A.8 Proof of Lemma 3.8

We first provide the following lemma.

Lemma A.5. (*David and Nagaraja [1970]*) *Let Φ be the cdf function of the standard normal distribution, then*

$$\lim_{n \rightarrow \infty} \Phi(a_n x + b_n)^n = e^{-\exp(-x)}, \quad (40)$$

where $b_n = \Phi^{-1}(1 - \frac{1}{n})$ and $a_n = \frac{1}{n\phi(b_n)}$.

For any j and for fixed μ_j and σ_{jj} , we standardized the x_{ij} 's and introduce $z_i = \frac{x_{ij} - \mu_j}{\sqrt{\sigma_{jj}}}$. Clearly z_1, \dots, z_n are i.i.d. standard normal random variables. Applying Lemma A.5, for any $\delta > 0$,

$$\lim_{n \rightarrow \infty} p(\max_{1 \leq i \leq n} z_i < a_n \delta + b_n) = e^{-\exp(-\delta)}.$$

Transforming z_i 's back to x_{ij} 's, we get

$$\lim_{n \rightarrow \infty} p \left[\max_{1 \leq i \leq n} x_{ij} < \sqrt{\sigma_{jj}} (a_n \delta + b_n) + \mu_j \right] = e^{-\exp(-\delta)}.$$

Since $y_{ij} = \mathbb{1}\{x_j > 0\}[x_{ij}]$, it is easily seen that for any $a \geq 0$, $\max_{1 \leq i \leq n} x_{ij} < a$ implies $\max_{1 \leq i \leq n} y_{ij} < a + 1$. Hence

$$p \left[\max_{1 \leq i \leq n} y_{ij} < \sqrt{\sigma_{jj}} (a_n \delta + b_n) + \mu_j + 1 \right] \geq p \left[\max_{1 \leq i \leq n} x_{ij} < \sqrt{\sigma_{jj}} (a_n \delta + b_n) + \mu_j \right]$$

holds for any n , which implies

$$\lim_{n \rightarrow \infty} pr \left[\max_{1 \leq i \leq n} y_{ij} < \sqrt{\sigma_{jj}} (a_n \delta + b_n) + \mu_j + 1 \right] \geq e^{-\exp(-\delta)}.$$

It is easily seen that $b_n \rightarrow \infty$. Using Mills ratio, we can show that for any $x > 0$, $\lim_{n \rightarrow \infty} \frac{1 - \Phi(b_n)}{\phi(b_n)} = \frac{1}{b_n}$. Noting that $1 - \Phi(b_n) = \frac{1}{n}$, we have shown that

$$\lim_{n \rightarrow \infty} a_n = \frac{1}{b_n}. \quad (41)$$

Integrating by parts, one can easily show the following two bounds:

$$1 - \Phi(x) \leq \frac{e^{-x^2/2}}{\sqrt{2\pi}x}, \quad 1 - \Phi(x) \geq \frac{e^{-x^2/2}}{\sqrt{2\pi}} \left(\frac{1}{x} - \frac{1}{x^3} \right).$$

Since $1 - \Phi(b_n) = \frac{1}{n}$, it can be shown that $\sqrt{2 \log n} \leq b_n \leq \sqrt{2 \log n}$ for sufficiently large n . Coupled with (41), we would have $a_n < \frac{2}{\sqrt{\log n}}$. This implies that

$$a_n \delta + b_n < \frac{2\delta}{\sqrt{\log n}} + \sqrt{2 \log n},$$

and hence

$$\begin{aligned} & pr \left[\max_{1 \leq i \leq n} y_{ij} < \sqrt{\sigma_{jj}} (a_n \delta + b_n) + \mu_j + 1 \right] \\ & < pr \left[\max_{1 \leq i \leq n} y_{ij} < \sqrt{\sigma_{jj}} \left(\frac{2\delta}{\sqrt{\log n}} + \sqrt{2 \log n} \right) + \mu_j + 1 \right], \end{aligned}$$

which completes the proof.

References

- H. Attias. A variational bayesian framework for graphical models. In *Advances in neural information processing systems*, pages 209–215, 2000.
- A. Canale and D. B. Dunson. Bayesian kernel mixtures for counts. *Journal of the American Statistical Association*, 106(496):1528–1539, 2011.
- D. R. Cox and N. Reid. A note on pseudolikelihood constructed from marginal densities. *Biometrika*, 91(3):729–737, 2004.
- H. A. David and H. N. Nagaraja. *Order statistics*. Wiley Online Library, 1970.
- K. El-Basyouny, S. Barua, and M. T. Islam. Investigation of time and weather effects on crash types using full Bayesian multivariate Poisson lognormal models. *Accident Analysis & Prevention*, 73:91–99, 2014.
- G. Folland. Higher-order derivatives and Taylor’s formula in several variables, 2005.
- A. Gelman et al. Prior distributions for variance parameters in hierarchical models (comment on article by Browne and Draper). *Bayesian analysis*, 1(3):515–534, 2006.
- J. K. Ghosh, M. Delampady, and T. Samanta. *An introduction to Bayesian analysis: theory and methods*. Springer Science & Business Media, 2007.
- T. S. Jaakkola and M. I. Jordan. Bayesian parameter estimation via variational methods. *Statistics and Computing*, 10(1):25–37, 2000.
- J. E. Johndrow, A. Smith, N. Pillai, and D. B. Dunson. Inefficiency of data augmentation for large sample imbalanced data. *arXiv preprint arXiv:1605.05798*, 2016.
- D. Lewandowski, D. Kurowicka, and H. Joe. Generating random correlation matrices based on vines and extended onion method. *Journal of multivariate analysis*, 100(9):1989–2001, 2009.
- J. Ma, K. M. Kockelman, and P. Damien. A multivariate Poisson-lognormal regression model for prediction of crash counts by severity, using Bayesian methods. *Accident Analysis & Prevention*, 40:964–975, 2008.

- F. Pauli, W. Racugno, and L. Ventura. Bayesian composite marginal likelihoods. *Statistica Sinica*, pages 149–164, 2011.
- H. Rue, S. Martino, and N. Chopin. Approximate bayesian inference for latent gaussian models by using integrated nested laplace approximations. *Journal of the royal statistical society: Series b (statistical methodology)*, 71(2):319–392, 2009.
- S. L. Scott, A. W. Blocker, F. V. Bonassi, H. A. Chipman, E. I. George, and R. E. McCulloch. Bayes and big data: The consensus Monte Carlo algorithm. *International Journal of Management Science and Engineering Management*, 11(2):78–88, 2016.
- J. Tang, J. Zhang, L. Yao, J. Li, L. Zhang, and Z. Su. Arnetminer: extraction and mining of academic social networks. In *Proceedings of the 14th ACM SIGKDD international conference on Knowledge discovery and data mining*, pages 990–998. ACM, 2008.
- X. Wang and D. B. Dunson. Parallelizing MCMC via Weierstrass sampler. *arXiv preprint arXiv:1312.4605*, 2013.